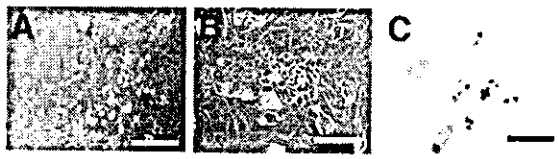

Fig. 4. Development of adherent hematopoietic cell clusters. (A,B) An adherent hematopoietic cell cluster (A) and a cluster with a cobblestone appearance that grew underneath the OP9 stromal cells (B). (C) Alkaline phosphatase staining of adherent hematopoietic cell clusters immunolabeled with human CD34 antibody. Scale bars: 100 μm.

exogenous EPO (Fig. 4A), and contained some typical cobblestone-like cells, which are known to be characteristic of immature hematopoietic progenitors (Fig. 4B). The adherent fraction has been reported to contain more progenitors than the floating fraction in the OP9 co-culture system (Suwabe et al., 1998). The number of clusters increased to a maximum on day 10, but rapidly decreased thereafter. Immunostaining demonstrated that more than half of the cells in the clusters were positive for CD34 (Fig. 4C).

Primitive erythroid colonies were generated from primate ES cells in methylcellulose colony-forming assays

To evaluate the generation of various progenitors in this system, we first performed methylcellulose colony-forming assays in the presence of a mixture of cytokines, including G-CSF, EPO, IL3, SCF and THPO, under stromal-free conditions using dissociated adherent cells with trypsin treatment. However, only a few granulocyte and macrophage colonies were observed (Fig. 5A,B), and erythroid colonies were never generated at any time during differentiation induction. To improve the system, the medium in the 6-well plates was sequentially replaced with a methylcellulose-containing medium that included a mixture of cytokines. Erythroid colonies were generated from the cultures replaced on day 7 of induction, with a peak on day 8 or day 9 (Fig. 5C,D). The number of erythroid colonies gradually decreased, and no colony formation was observed from day 12 and thereafter. The colonies were first identified 5 days after the addition of methylcellulose-containing medium. Immunostaining demonstrated that all the erythrocytes in the colonies were positive for Hb, HbF and HbEmb (Fig. 5E,F), corresponding to EryP. All 10 of the representative erythroid colonies examined expressed not only embryonic (ε and ζ), but also fetal (γ) or adult (β and α) globin genes (Fig. 5G). These results suggest that the erythroid colonies were derived from primitive hematopoiesis.

Flow cytometric and RT-PCR analysis of hematopoietic development in the OP9 co-culture system

To investigate whether the temporal expression pattern of genes involved in hematopoietic development is also reproduced in the OP9 co-culture system, we first examined the expression of KIT, FLK1 and CD34, which are surface markers expressed by early hematopoietic cells. As shown in Fig. 6, flow cytometric analysis of undifferentiated ES cells revealed that almost all cells expressed KIT and FLK1, although CD34-positive cells were not detected. The expression of KIT and FLK1 declined on day 4, but was upregulated on day 6. CD34-positive cells were first observed on day 6, and increased thereafter.

We also examined the expression of genes associated with hematopoietic development by RT-PCR (Fig. 7). Brachyury, an early mesodermal marker, was expressed on day 4 but its expression declined on day 6. The expression of FLK1, LMO2, MYB and GATA2, which were detected in undifferentiated ES cells, declined on day 4, but was upregulated on day 6, just before hematopoietic development. SCL expression was first detected on day 6 and remained constant thereafter. By contrast, the marker genes that are indicative of ectoderm (Nestin), endoderm (AFP), and undifferentiated ES cells (REX1) were expressed during differentiation induction. Altogether, these results suggest that the hematopoietic development that is induced in the co-culture system parallels

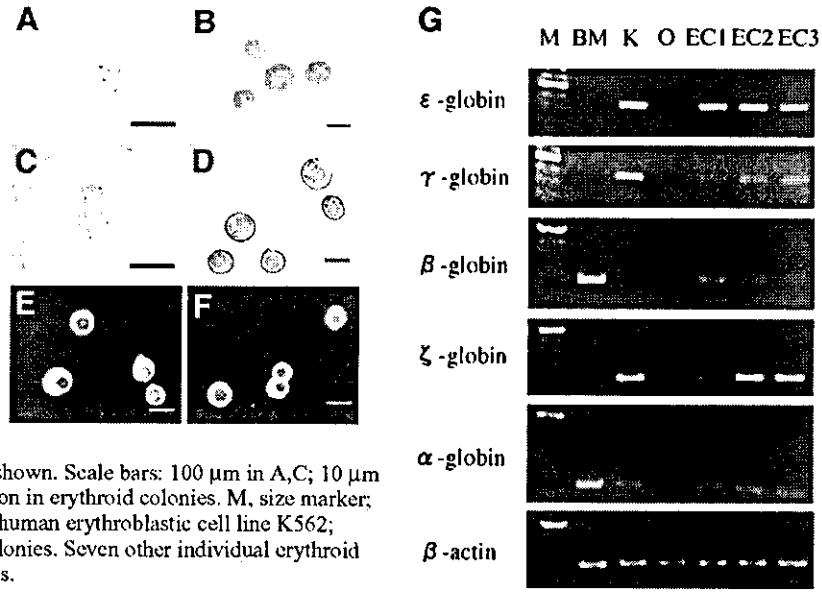

Fig. 5. Development of hematopoietic colonies. Methylcellulose colony-forming assays were performed on day 8. Using adherent cells dissociated with trypsin treatment, only a few GM colonies were observed (A,B). When the medium was replaced with methylcellulose-containing medium, erythroid colonies were generated on the OP9 stromal cell layer (C-F). (A,C) Morphology of a GM colony (A) and a primitive erythroid colony (C). (B,D) May-Giemsa staining of a GM colony (B) and a primitive erythroid colony (D). (E,F) Human hemoglobin (Hb; FITC) and fetal hemoglobin (Cy3; E), and Hb (FITC) and embryonic hemoglobin (Cy3; F) staining of erythrocytes in a primitive erythroid colony. Nuclei were labeled with Hoechst 33342. Merged images are shown. Scale bars: 100 μm in A,C; 10 μm in B,D-F. (G) RT-PCR analysis of globin gene expression in erythroid colonies. M, size marker; BM, adult cynomolgus monkey bone marrow cells; K, human erythroblastic cell line K562; O, OP9 stromal cells; EC1-EC3, primitive erythroid colonies. Seven other individual erythroid colonies showed similar globin gene expression patterns.

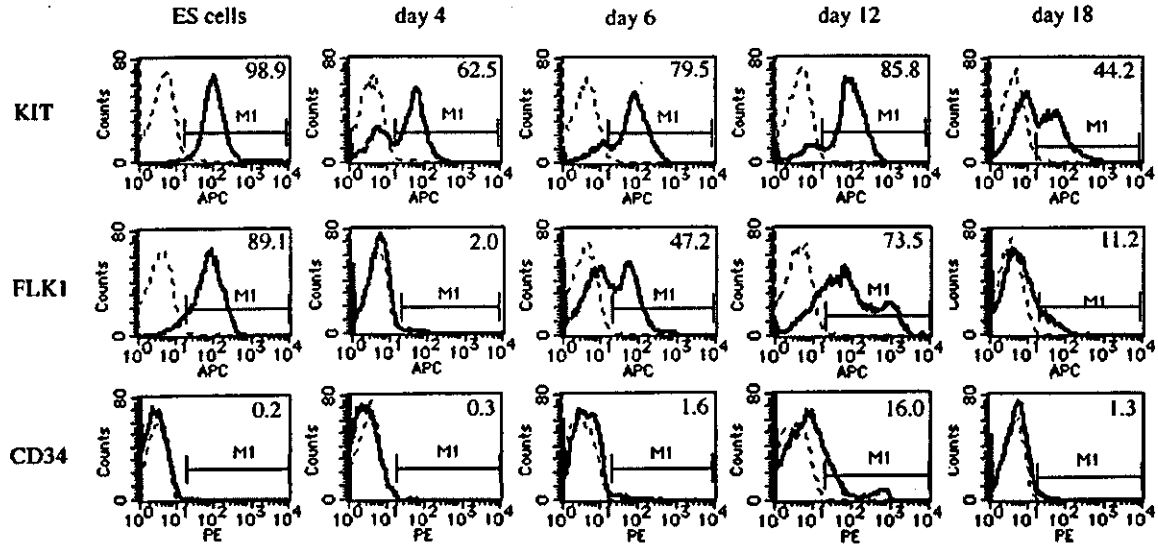

Fig. 6. Sequential flow cytometric analysis of KIT, FLK1 and CD34 during differentiation induction. Undifferentiated ES cells, or the cultures on day 4, 6, 12 and 18, were stained with antibodies specific for KIT, FLK1 or CD34, or with control IgG1. Plots show the isotype control IgG1 staining profile (dashed lines) versus the specific antibody staining profiles (solid lines). Representative results from one of three independent experiments are shown.

that found in the embryo, and that the development of other lineages also occurred concomitantly.

VEGF enhances primitive and definitive hematopoiesis in a dose-dependent manner in the OP9 co-culture system and methylcellulose assay

Although the transition from primitive to definitive hematopoiesis was induced, definitive hematopoiesis was less efficient in our culture system, irrespective of exogenous EPO. As VEGF, bFGF, and BMP4 have been shown to promote primitive and definitive hematopoietic development in murine ES cells (Johansson and Wiles, 1995; Faloon et al., 2000; Nakayama et al., 2000), we tested these growth factors in our culture system.

Exogenous VEGF increased the number of erythrocytes in a dose-dependent manner until day 14, in the presence or absence of EPO (Fig. 8A). These erythrocytes consisted exclusively of EryP. EryD were rarely observed in the presence of VEGF alone (data not shown), whereas exogenous VEGF plus EPO enhanced EryD production more prominently with time (Fig. 8B).

The total number of hematopoietic cells was increased by exogenous VEGF irrespective of the presence of EPO (Fig. 8C). VEGF did not affect the percentage of each lineage population (Fig. 8D), and the increase in myeloid cells, major components of definitive hematopoiesis, contributed to the increase of the total number of hematopoietic cells after day 14. Furthermore, exogenous VEGF enhanced the increase in both adherent cell clusters and primitive erythroid colonies in a dose-dependent manner (Fig. 8E,F), suggesting that VEGF affects hematopoiesis at the progenitor level. Exogenous bFGF did not alter the process of hematopoiesis, or the number of adherent clusters and erythroid colonies. By contrast, exogenous BMP4 exerted an adverse effect on hematopoiesis (Fig. 8E-H).

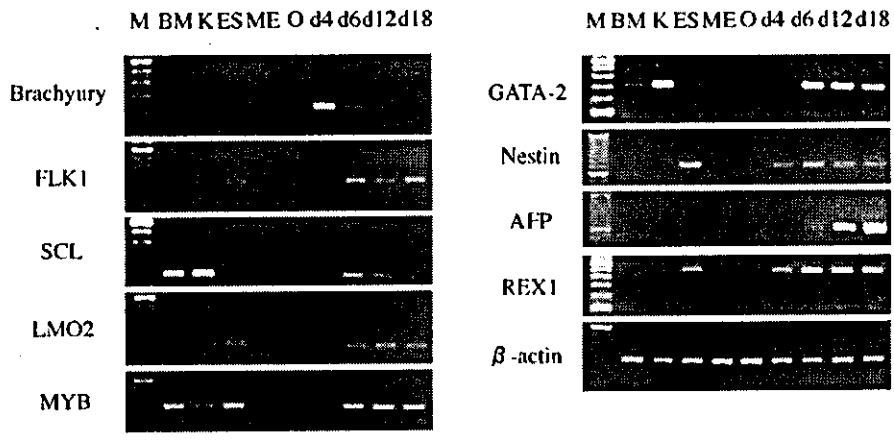

Fig. 7. Sequential RT-PCR analysis of genes associated with hematopoietic development in cultures during liquid culture differentiation. M, size marker; BM, adult cynomolgus monkey bone marrow cells; K, human erythroblastic cell line K562; ES, undifferentiated ES cells; ME, mouse embryonic fibroblasts; O, OP9 stromal cells; d, days after the induction of differentiation in the presence of EPO.

More efficient primitive and definitive hematopoiesis is induced by re-plating sorted CD34-positive cells

As previously shown, other lineages developed concomitantly in our culture system. Consequently, we purified the CD34-positive cells in the cultures and seeded them onto fresh OP9 stromal cells on day 10 (Fig. 9A-

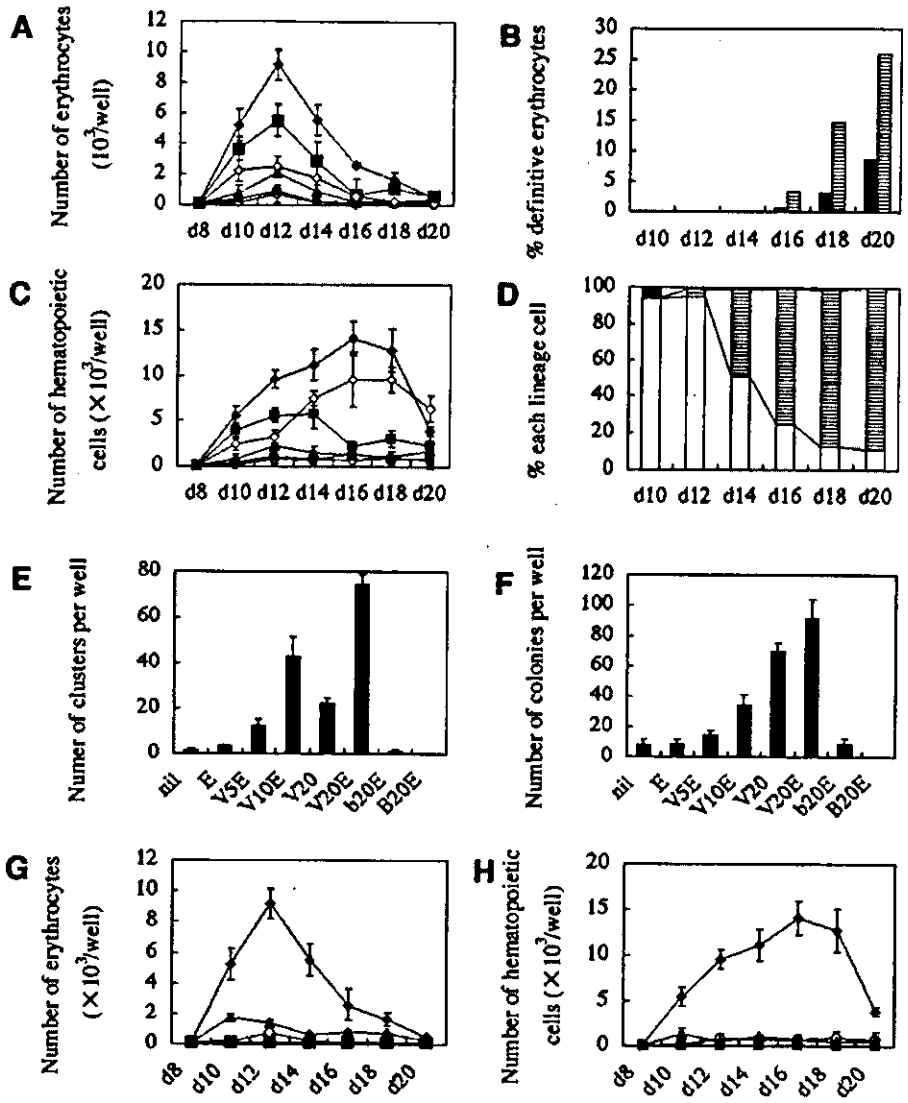

Fig. 8. Effects of EPO and various growth factors on primitive and definitive hematopoiesis. Primate ES cells were cultured for 6 days with VEGF, bFGF or BMP4. The induced cells were harvested and re-cultured with (black circles) or without (white circles) 10 U/ml EPO. The floating cells were analyzed as described in Fig. 2. Adherent clusters (≥20 cells) were counted on day 10. Primitive erythroid colonies (≥50 cells) were counted 7 days after replacing the medium with methylcellulose-containing medium on day 8. (A,C) Effects of EPO and various concentrations of VEGF (0 ng/ml, circles; 5 ng/ml, triangles; 10 ng/ml, squares; 20 ng/ml, diamonds) on the number of erythrocytes (A) and total hematopoietic cells (C). (B) Sequential analysis of the proportion of definitive erythrocytes (EryD) among total erythrocytes in the presence of EPO alone (black columns), or EPO plus VEGF (20 ng/ml; striped columns). (D) Sequential analysis of the percentages of erythrocytes (white columns), myeloid cells (striped columns) and megakaryocytes (black columns) among total hematopoietic cells in the presence of EPO plus VEGF (20 ng/ml). (E,F) Effects of EPO and growth factors on the number of adherent hematopoietic clusters (E) and primitive erythroid colonies (F). E, EPO; V, VEGF (5 to 20 ng/ml); b, bFGF (20 ng/ml); B, BMP4 (20 ng/ml). (G,H) Effects of bFGF (20 ng/ml, triangles), BMP4 (20 ng/ml, squares) and VEGF (20 ng/ml, diamonds) on the number of erythrocytes (G) and total hematopoietic cells (H). Data represent the mean±s.d. of triplicate wells. Representative results from one of three independent experiments are shown.

C). In the presence of EPO, approximately on day 25 (i.e. 15 days after the cell sorting), adherent hematopoietic cell clusters grew larger and had a cobblestone appearance (Fig. 9D). The number of floating cells, most of which were erythrocytes, increased with a peak on day 28 (Fig. 9E,H,I). Nearly 40% of these erythrocytes were definitive, and many were enucleated (Fig. 9E-G,J,K). In the absence of EPO, hematopoietic development after cell sorting was barely observed. These results indicate that CD34-positive cells in cultures contained progenitors of both primitive and definitive hematopoiesis.

Discussion

In this study, we have demonstrated that nonhuman primate ES cells are a suitable tool for dissecting the molecular and cellular mechanisms of primitive and definitive hematopoietic development. The capacity of murine ES cells to differentiate into hematopoietic cells has been investigated intensively in many culture systems (Doestchmann et al., 1985; Wiles and Keller, 1991; Keller et al., 1993; Nakano et al., 1996; Nishikawa et al., 1998); in particular, the transition from primitive to definitive hematopoiesis can be induced in murine ES cells by co-culture on OP9 stromal cells in vitro (Nakano et al., 1996). This culture system can reproduce hematopoietic development from murine ES cells with a pattern similar to that observed in developing mouse embryos, and has been established as a powerful experimental tool for elucidating the regulation of hematopoietic development and differentiation (Suwabe et al., 1998; Era et al., 2000; Kitajima et al., 2002).

The hematopoietic development of primates, however, is different from that of mice. For example, expression of the γ gene during the fetal period is an event that occurs only among primates (TomHon et al., 1997). Therefore, in vitro and in vivo studies of primate hematopoietic development should be performed using primate-derived materials. In recent studies in primate ES cells, Kaufman et al. and Li et al. demonstrated that the definitive hematopoiesis, but not the primitive hematopoiesis, of in vivo differentiation is recapitulated (Kaufman et al., 2001; Li et al., 2001). Lu et al. revealed that

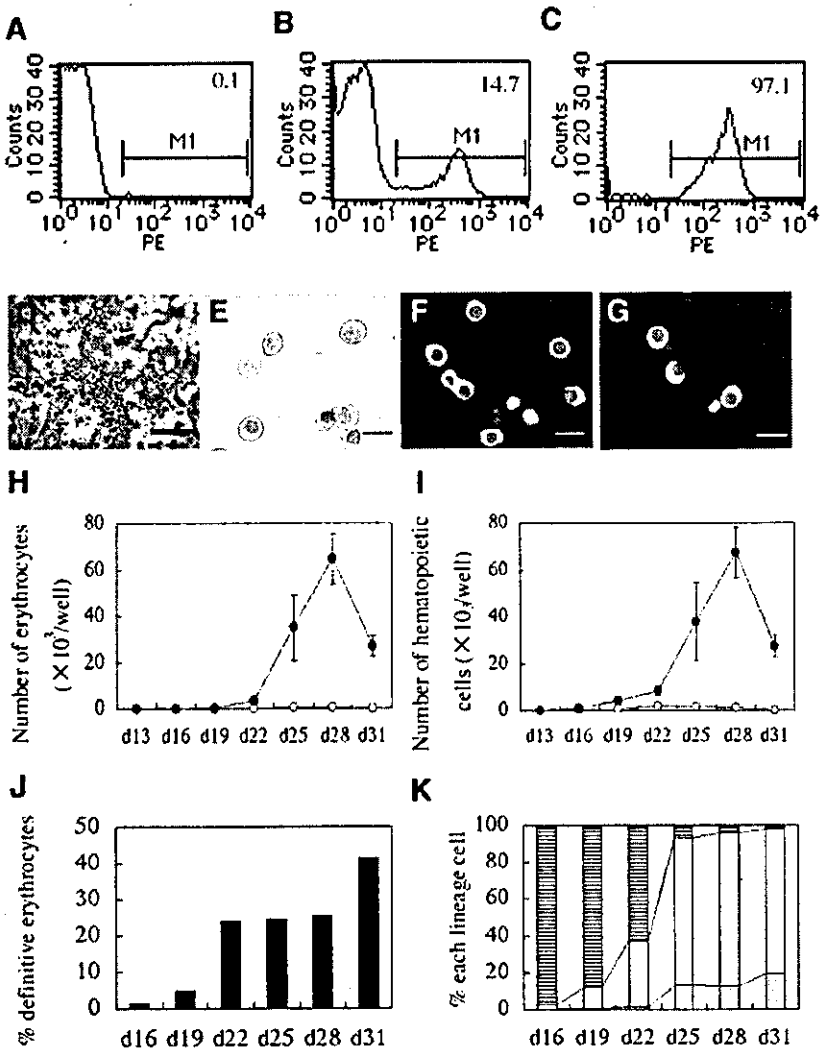

Fig. 9. More efficient primitive and definitive hematopoiesis is induced by re-plating sorted CD34-positive cells. (A-C) Flow cytometric analysis and cell sorting of cultures on day 10 with human CD34 antibody. A sorting gate in B was defined according to the intensity of staining with an isotype control antibody (A). Reanalysis of the sorted cells confirmed the purity as 95 to 98% (C). (D) Large adherent hematopoietic cell cluster with a cobblestone appearance on day 25. Scale bars: 100 μm. (E-G) May-Giemsa staining (E), human hemoglobin (Hb; FITC) and embryonic hemoglobin (Cy3; F), and Hb (FITC) and fetal hemoglobin (Cy3; G) staining of day 25 erythrocytes grown in the presence of EPO. Nuclei were labeled with Hoechst 33342. Merged images are shown. Scale bars: 10 μm. (H,I) Sequential analysis of the number of erythrocytes (H) and total hematopoietic cells (I), with (black circles) or without (white circles) 10 U/ml EPO. (J) Sequential analysis of the proportion of definitive erythrocytes among total erythrocytes. (K) Sequential analysis of the percentages of enucleated erythrocytes (stippled columns), nucleated erythrocytes (white columns) and myeloid cells (striped columns) in the presence of EPO. Data represent the mean+s.d. of triplicate wells. Representative results from one of three independent experiments are shown.

the coexistence of primitive and definitive hematopoiesis is recapitulated at the mRNA level (Lu et al., 2002). In this study, we have demonstrated for the first time the transition from primitive to definitive hematopoietic development in primate ES cells at both the transcriptional and the translational level in vitro. Immunostaining using human hemoglobin antibodies demonstrates that embryonic and definitive (fetal) erythrocytes appear on day 8 and day 16, respectively. Sequential RT-PCR analysis of globin genes demonstrates upregulation of primitive (ε and ζ) globin gene expression on day 8 and of definitive (γ and α) globin genes on day 12, which indicates that the erythropoietic transition can be recapitulated in ES cells at the mRNA level. Therefore, our in vitro system is superior in precisely reflecting the ontogeny of hematopoietic cells in vivo, and should be a useful tool to define the mechanisms of primate hematopoiesis. The generation of adherent hematopoietic cell clusters containing CD34-positive cells onto the OP9 cell layer indicates that this induction system also recapitulates hematopoietic development at the progenitor level from primate ES cells, as has been observed in murine ES cells (Nakano et al., 1996; Suwabe et al., 1998; Era et al., 2000; Kitajima et al., 2002).

Our results from the colony assays also demonstrate for the first time that primitive erythroid colonies are generated with the aid of stromal cells, but that definitive colonies do not emerge in the presence or absence of stromal cells. By contrast, a recent study has shown that definitive erythroid colonies are generated from primate ES cells under stromal-free conditions, but that primitive colonies are not (Kaufman et al., 2001). These differences may be partially due to differences in the culture conditions, the colony assays, and/or the ES cells and stromal cells that were used for the induction of differentiation. Notably, our individual primitive erythroid colonies express not only embryonic but also fetal and adult globin genes, which is consistent with the results obtained by plating human embryonic or fetal cells (Peschle et al., 1984; Stamatoyannopoulos et al., 1987). Fetal and adult hemoglobin synthesis, and factors regulating their synthesis, have been intensively analyzed in human cord blood, and in neonatal and adult erythroid colonies (Stamatoyannopoulos et al., 2001). However, precise analysis of hemoglobin synthesis in primitive erythroid colonies has not been performed. Thus, our culture system will also serve as a powerful tool for elucidating the regulatory mechanisms of primitive hematopoiesis.

Co-culture on OP9 stromal cells alone induces hematopoietic development less efficiently in primate ES cells than in murine ES cells. VEGF, bFGF and BMP4 have been reported to promote primitive or definitive hematopoietic development in previous studies in murine ES cells (Johansson and Wiles, 1995; Faloon et al., 2000; Nakayama et al., 2000). Therefore, we quantified the stimulatory effects of these

growth factors on both types of hematopoiesis. Unexpectedly, exogenous BMP4 fails to induce hematopoietic differentiation in our culture system. There are two possible explanations for this discrepancy. One is that human BMP4 does not work on the cynomolgus ES cell line we used. However, considering that human BMP4 functions in both murine and primate ES cells (Johansson and Wiles, 1995; Nakayama et al., 2000; Li et al., 2001; Chadwick et al., 2003) the possibility seems unlikely. Another possibility is that BMP4 causes the OP9 stromal cells to differentiate and thereby impairs their interaction with ES cells. Supporting this notion is the fact that we observed that exogenous BMP4 resulted in an increase of adipocytes on the OP9 cell layer (data not shown). This observation is also consistent with a previous report that showed that BMP4 induces the differentiation of mesenchymal progenitors into distinct various mesenchymal cell lineages including adipocytes (Ahrens et al., 1993).

Of course, there is a common requirement for cytokines or growth factors during hematopoietic differentiation from both primate and murine ES cells. We demonstrated that in primate erythropoiesis, exogenous EPO is required for EryD development, whereas EryP develop independently of EPO, despite substantial expression of EPO receptor. This result is consistent with reports showing that murine primitive and definitive erythrocytes have different requirements for EPO (Wu et al., 1995; Lin et al., 1996). As previously reported in murine ES cells (Heberlein et al., 1992; Keller et al., 1993), the EPOR is expressed in undifferentiated primate ES cells. However, it is unlikely that erythrocytes are contained in undifferentiated ES cells, because no globin gene expression is detected before the induction of differentiation. Further studies will be required to analyze the function of EPOR expressed in undifferentiated ES cells.

Among growth factors examined in this study, VEGF, a ligand for FLK1, was the only one to stimulate both primitive and definitive hematopoiesis. FLK1 is required for the development of primitive and definitive hematopoietic cells, as well as endothelial cells, in the murine embryo (Shalaby et al., 1995; Shalaby et al., 1997). Recent studies on the differentiation of murine ES cells in vitro also indicate that primitive and definitive hematopoietic and endothelial cell lineages can be generated from FLK1-positive cells (Choi et al., 1998; Nishikawa et al., 1998; Faloon et al., 2000). In our study, the expression of FLK1 was upregulated on day 6, before hematopoietic development. This result is consistent with the recent report on vascular progenitor cell differentiation from cynomolgus monkey ES cells onto OP9 stromal cells (Sone et al., 2003). Furthermore, we observed that exogenous VEGF also enhances the development of vascular endothelial cadherin-positive endothelial colonies under the same culture conditions (K.U., T.H. and T.N., unpublished). Taken together, these results strongly suggest that primitive and definitive hematopoietic, as well as endothelial, lineage progenitors are derived from FLK1-positive cells in culture. Further studies, by single cell culture of FLK1-positive cells to differentiate into both lineage cells, will be needed to confirm this possibility.

We also examined indispensable genes associated with hematopoietic development. GATA2 has been reported to be necessary for the proliferation and survival of both primitive and definitive hematopoietic progenitors (Tsai et al., 1994). Its expression in our system supports the proposed role it plays in the generation of hematopoietic progenitors. The expression of Brachyury, an early mesodermal marker (Herrmann et al., 1994), was upregulated on day 4, and was followed by the upregulation of SCL, MYB and LMO2 expression on day 6, before hematopoietic development. SCL (Robb et al., 1996; Porcher et al., 1996) and LMO2 (Warren et al., 1994; Yamada et al., 1998) are required for both primitive and definitive hematopoietic development, whereas MYB is essential for the development of definitive hematopoiesis only (Mucenski et al., 1991). SCL is also crucial for the development of hemangioblasts (Faloon et al., 2000; Chung et al., 2002). These results suggest that a similar profile of genes is involved in hematopoiesis in culture as is involved in early hematopoiesis in vivo. These observations will also facilitate the genetic manipulations of ES cells that may shed light on the unresolved molecular mechanisms behind hematopoietic development.

As sequential RT-PCR analysis of Nestin, AFP and REX1 indicated that other lineage cells and undifferentiated ES cells also grow during the differentiation induction process, we purified the CD34-positive cells in the cultures and seeded them onto fresh OP9 stromal cells. Analyses after cell sorting indicated that enhanced definitive hematopoiesis was generated on day 25 and thereafter, although primitive hematopoiesis was still produced. These results indicate that both hematopoietic processes originate from the sorted CD34-positive population. Further experiments to quantitatively analyze definitive hematopoiesis will be performed using this improved assay.

In conclusion, the sequential development of primitive and definitive hematopoiesis can be induced from primate ES cells by co-culture with OP9 stromal cells. This induction system will provide new approaches for elucidating the mechanisms regulating primate hematopoietic development and differentiation during embryogenesis.

We would like to thank Tanabe Seiyaku Co. Ltd. (Osaka, Japan), for help in primate ES cell preparation, and Ken-ichi Suzuki (Yamanouchi Seiyaku) for providing cynomolgus monkey bone marrow cells. We also thank Drs T. Yasumi, R. Nishikomori and M. Ogawa for critical reading of the manuscript. This study was supported by grants from the Scientific Research on Priority Areas, the Creative Science Research, the Japan Society for the Promotion of Science, and the Ministry of Education, Culture, Sports, Science and Technology.

References

Ahrens, M., Ankenbauer, T., Schroder, D., Hollnagel, A., Mayer, H. and Gross, G. (1993). Expression of human bone morphogenetic proteins -2 or -4 in murine mesencymal progenitor C3H10T1/2 cells induces differentiation into distinct mesencymal cell lineages. *DNA Cell Biol.* **12**, 871-880.

Chadwick, K., Wang, L., Li, L., Menendez, P., Murdoch, B., Rouleau, A. and Bhatia, M. (2003). Cytokines and BMP-4 promote hematopoietic differentiation of human embryonic stem cells. *Blood* **102**, 906-915.

Choi, K., Kennedy, M., Kazarov, A., Paradimitrou, J. C. and Keller, G. (1998). A common precursor for hematopoietic and endothelial cells. *Development* **125**, 725-732.

Chung, Y. S., Zhang, W. J., Arentson, E., Kingsley, P. D., Palis, J. and Choi, K. (2002).Lineage analysis of the hemangioblast as defined by FLK1 and SCL expression. *Development* **129**, 5511-5520.

Doetschmann, T. C., Eistetter, H., Katz, M., Schmidt, M. and Kemler, R. (1985). The in vitro development of blastocyst-derived embryonic stem cell lines: formation of visceral yolk sac, blood islands and myocardium. *J. Embryol. Exp. Morphol.* **87**, 27-45.

Dzierzak, E. and Medvinsky, A. (1995). Mouse embryonic hematopoiesis. *Trends. Genet.* **11**, 359-366.

Era, T., Takagi, T., Takahashi, T., Bories, J. C. and Nakano, T. (2000). Characterization of hematopoietic lineage-specific gene expression by ES cell in vitro differentiation induction system. *Blood* **95**, 870-878.

Faloon, P., Arentson, E., Kazarov, A., Deng, C. X., Porcher, C., Orkin, S. and Choi, K. (2000). Basic fibroblast growth factor positively regulates hematopoietic development. *Development* **127**, 1931-1941.

Hanazono, Y., Terao, K. and Ozawa, K. (2000). Gene transfer into nonhuman primate hematopoietic stem cells: implication for gene therapy. *Stem Cells* **19**, 12-23.

Heberlein, C., Fischer, K. D., Stoffel, M., Nowock, J., Ford, A., Tessmer, U. and Stocking, C. (1992). The gene for erythropoietin receptor is expressed in multipotential hematopoietic and embryonic stem cells: evidence for differentiation stage-specific regulation. *Mol. Cell. Biol.* **12**, 1815-1826.

Herrmann, B. G. and Kispert, A. (1994). The T genes in embyogenesis. *Trends Genet.* **10**, 280-286.

Johansson, B. M. and Wiles, M. V. (1995). Evidence for involvement of activin A and bone morphogenetic protein 4 in mammalian mesoderm and hematopoietic development. *Mol. Cell. Biol.* **15**, 141-151.

Johnson, R. M., Buck, S., Chiu, C. H., Gage, D. A., Shen, T. L., Hendrickx, A. G., Gumucio, D. L. and Goodman, M. (2000). Humans and Old World monkeys have similar patterns of fetal globin expression. *J. Exp. Zool. (Mol. Dev. Evol.)* **288**, 318-326.

Kaufman, D. S., Hanson, E. T., Lewis, R. L., Auerbach, R. and Thomson, J. A. (2001).Hematopoietic colony-forming cells derived from human embryonic stem cells. *Proc. Natl. Acad. Sci. USA* **98**, 10716-10721.

Keller, G., Kennedy, M., Papayannopoulou, T. and Wiles, M. V. (1993). Hematopoietic commitment during embryonic stem cell differentiation in culture. *Mol. Cell. Biol.* **13**, 473-486.

Kitajima, K., Masuhara, M., Era, T., Enver, T. and Nakano, T. (2002). GATA-2 and GATA-2/ER display opposing activities in the development and differentiation of blood progenitors. *EMBO J.* **21**, 3060-3069.

Li, F., Lu, S., Vida, L., Thomson, J. A. and Honig, G. R. (2001). Bone morphogenetic protein 4 induces efficient hematopoietic differentiation of rhesus monkey embryonic stem cells in vitro. *Blood* **98**, 335-342.

Lin, C. S., Lim, S. K., D'Agati, V. and Constantini, F. (1996). Differential effects of an erythropoietin receptor gene disruption on primitive and definitive erythropoiesis. *Genes Dev.* **10**, 154-164.

Lu, S. J., Quan, C., Li, F., Vida, L. and Honig, G. R. (2002). Hematopoietic progenitor cells derived from embryonic stem cells: analysis of gene expression. *Stem Cells* **20**, 428-437.

Luo, H. Y., Liang, X. L., Frye, C., Wonio, M., Hankins, D. H. K. and Alter, B. P. (1999). Embryonic hemoglobins are expressed in definitive cells. *Blood* **94**, 359-361.

Mucenski, M. L., Mclain, K., Kier, A. B., Sweldlow, S. H., Schreiner, C. M. Miller, T. A., Pietryga, D. W., Scott, W. J. and Potter, S. S. (1991). A functional C-myb is required for normal murine fetal hepatic hematopoiesis. *Cell* **65**, 677-689.

Nakahata, T. and Ogawa M. (1982). Hemopoietic colony-forming cells in umbilical cord blood with extensive capacity to generate mono- and multipotential hemopoietic progenitors. *J. Clin. Invest.* **70**, 1324-1328.

Nakano, T., Kodama, H. and Honjo, T. (1996). In vitro development of primitive and definitive erythrocytes from different precursors. *Science* **272**, 722-724.

Nakayama, N., Lee, J. and Chiu, L. (2000). Vascular endothelial growth factor synergistically enhances bone morphogenetic protein-4-dependent lymphohematopoietic cell generation from embryonic stem cells in vitro. *Blood* **95**, 2275-2283.

Nishikawa, S. I., Nishikawa, S., Hirashima, M. and Matsuyoshi, N. (1998). Progressive lineage analysis by cell sorting and culture identifies FLK1$^+$VE-cadherin$^+$ cells at a diverging point of endothelial and hemopoietic lineages. *Development* **125**, 1747-1757.

Porcher, C., Swat, W., Rockwell, K., Fujiwara, Y., Alt, F. W. and Orkin, S. H. (1996). The T cell leukemia oncoprotein SCL/tal-1 is essential for development of all hematopoietic lineages. *Cell* **86**, 47-57.

Peschle, C., Migliaccio, A. R., Migliaccio, G., Petrini, M., Calandrini, M., Russo, G., Mastroberardio, G., Presta, M., Gianni, A. M., Comi, P. et al. (1981). Embryonic → fetal Hb switch in humans: studies on erythroid bursts generated by embryonic progenitors from yolk sac and liver. *Proc. Natl. Acad. Sci. USA* **78**, 348-352.

Robb, L., Elwood, N. J., Elefanty, A. G., Kontgen, F., Li, R., Barnett, L. D. and Begley, C. G. (1996). The scl gene product is required for the generation of all hematopoietic lineages in the adult mouse. *EMBO J.* **21**, 3060-3069.

Rutherford, T., Clegg, J. B., Higgs, D. R., Jones, R. W., Thompson, J. and Weatherrall, D. J. (1981). Embryonic erythroid differentiation in the human leukemic cell line K562. *Proc. Natl. Acad. Sci. USA* **78**, 348-352.

Sawano, A., Iwai, S., Sakurai, Y., Ito, M., Shitara, K., Nakahata, T. and Shibuya, M. (2001). Flt-1, vascular endothelial growth factor receptor 1, is a novel cell surface marker for the lineage of monocyte-macrophages in humans. *Blood* **97**, 785-791.

Schuldnier, M., Yanuka, O., Itskovitz-Eldor, J., Melton, D. A. and Benvenisty, N. (2000). Effects of eight growth factors on the differentiation of cells derived from human embryonic stem cells. *Proc. Natl. Acad. Sci. USA* **97**, 11307-11312.

Shalaby, F., Rossant, J., Yamaguchi, T. P., Gertsenstein, M., Wu, X. F., Breitman, M. L. and Schuh, A. C. (1995). Failure of blood-island formation and vasculogenesis in Flk-1 deficient mice. *Nature* **376**, 62-66.

Shalaby, F., Ho, J., Stanford, W. L., Fischer, K. D., Schuh, A. C., Schwartz, L., Bernstein, A. and Rossant, J. (1997). A requirement for Flk1 in primitive and definitive hematopoiesis and vasculogenesis. *Cell* **89**, 981-990.

Sone, M., Itoh, H., Yamashita, J., Yurugi-Kobayashi, T., Suzuki, Y., Kondo, Y., Nonoguchi, A., Sawada, N., Yamahata, K., Miyashita, K. et al. (2003). Different differentiation kinetics of vascular progenitor cells in primate and mouse embryonic stem cells. *Circulation* **107**, 2085-2088.

Stamatoyannopoulos, G. and Grosveld, F. (2001). Hemoglobin Switching. In *The Molecular Basis of Blood Disease* (ed. G. Stamatoyannopoulos, P. Majerus, R. M. Perlmutter and H. Varmus), pp. 135-182. Philadelphia: W. B. Saunders.

Stamatoyannopoulos, G., Constantoulakis, P., Brice, M., Kurachi, S. and Papayannopoulou, T. H. (1987). Coexpression of embryonic, fetal, and adult globins in erythroid cells of human embryos: relevance to the cell-lineage models of globin switching. *Dev. Biol.* **123**, 191-197.

Suemori, H., Tada, T., Torii, R., Hosoi, Y., Kobayashi, K., Imahie, H., Kondo, Y., Iritani, A. and Nakatsuji, N. (2001). Establishment of embryonic stem cell lines from cynomolgus monkey blastocysts produced by IVF or ICSI. *Dev. Dyn.* **222**, 273-279.

Sui, X., Tsuji, K., Tanaka, R., Tajima, S., Muraoka, K., Ebihara, Y., Ikebuchi, K, Yasuoka, K., Taga, T., Kishimoto, T. and Nakahata, T. (1995). gp130 and c-kit signalings synergize for ex vivo expansion of human primitive hemopoietic progenitor cells. *Proc. Natl. Acad. Sci. USA* **92**, 2859-2863.

Suwabe, N., Takahashi, S., Nakano, T. and Yamamoto, M. (1998). GATA-1 regulates growth and differentiation of definitive erythroid lineage cells during in vitro ES cell differentiation. *Blood* **92**, 4108-4118.

Tajima, S., Tsuji, K., Ebihara, Y., Sui, X., Tanaka, R., Muraoka, K., Yoshida, M., Yamada, K., Yasuoka, K., Taga, T., Kishimoto, T. and Nakahata, T. (1996). Analysis of interleukin 6 receptor and gp130 expressions and proliferative capability of human CD34$^+$ cells. *J. Exp. Med.* **184**, 1357-1364.

Tavian, M., Coulombel, L., Luton, D., Clemente, H. S., Dieterlen-Lievere, F. and Peault, B. (1996). Aorta-associated CD34$^+$ hematopoietic cells in the early human embryo. *Blood* **87**, 67-72.

Tavian, M., Hallais, M. F. and Peault, B. (1999). Emergence of intraembryonic hematopoietic precursors in the pre-liver human embryo. *Development* **126**, 793-803.

Thomson, J. A., Kalishman, J., Golos, T. G., Durning, M., Harris, C. P., Becker, R. A. and Hearn, J. P. (1995). Isolation of a primate embryonic stem cell line. *Proc. Natl. Acad. Sci. USA* **98**, 10716-10721.

Thomson, J. A., Kalishman, J., Golos, T. G., Durning, M., Harris, C. P. and Hearn, J. P. (1996). Pluripotent cell lines derived from common marmoset (Callithrix jacchublastocysts). *Biol. Reprod.* **55**, 254-259.

Thomson, J. A., Itskovitz-Eldor, J., Shapiro, S. S., Waknitz, M. A., Swiergiel, J. J., Marshall, V. S. and Jones, J. M. (1998). Embryonic stem cell lines derived from human blastocysts. *Science* **282**, 1145-1147.

Tomhon, C., Zhu, W., Millinoff, D., Hayasaka, K., Slightom, J. L., Goodman, M. and Gumucio, D. L. (1997). Evolution of a fetal expression pattern via *cis* changes near the γ globin gene. *J. Biol. Chem.* **272**, 14062-14066.

Tsai, F. Y., Keller, G., Kuo, F. C., Weiss, M., Chen, J., Rosenblatt, M., Alt, F. W. and Orkin, S. H. (1994). An early haematopoietic defect in mice lacking the transcriptional factor GATA-2. *Nature* **371**, 221-226.

Warren, A. J., Colledge, W. H., Carlton, M. B. L., Evans, M. J., Smith, A. J. H. and Rabbits, T. H. (1994). The oncogenic cysteine-rich LIM domain protein Rbtn2 is essential for erythroid development. *Cell* **78**, 45-57.

Wiles, M. V. and Keller, G. (1991). Multiple hematopoietic lineage

develop from embryonic stem (ES) cells in culture. *Development* **111**, 259-267.

Wu, H., Liu, X., Jaenisch, R. and Lodish, H. F. (1995). Generation of committed erythroid BFU-E and CFU-E progenitors does not require erythropoietin or the erythropoietin receptor. *Cell* **83**, 59-67.

Xu, M. J., Matsuoka, S., Yang, F. C., Ebihara, Y., Manabe, A., Tanaka, R., Eguchi, M., Asano, S., Nakahata, T. and Tsuji, K. (2001). Evidence for the presence of murine primitive megakarycytopoiesis in the early yolk sac. *Blood* **97**, 2016-2022.

Yamada, Y., Warren, A. J., Dobson, C., Foster, A., Pannell, R. and Rabbits, T. H. (1998).The T cell leukemia LIM protein Lmo2 is necessary for adult mouse hematopoiesis. *Proc. Natl. Acad. Sci. USA* **95**, 3890-3895.

Yokomizo, R., Matsuzaki, S., Uehara, S., Murakami, T., Yaegashi, N. and Okamura, K. (2002). Erythropoietin and erythropoietin receptor expression in human endometrium throughout the menstrual cycle. *Mol. Hum. Reprod.* **8**, 441-446.

Yoshida, H., Hayashi, S. I., Kunisada, T., Ogawa, M., Nishikawa, S., Okamura, H., Sudo, T., Shultz, L. D. and Nishikawa, S. I. (1990). The mutation osteopetrosis is in the coding region of the macrophage colony stimulating factor gene. *Nature* **345**, 442-444.

Complete reconstitution of human lymphocytes from cord blood CD34$^+$ cells using the NOD/SCID/γ_c^{null} mice model

Hidefumi Hiramatsu, Ryuta Nishikomori, Toshio Heike, Mamoru Ito, Kimio Kobayashi, Kenji Katamura, and Tatsutoshi Nakahata

Establishment of an assay capable of generating all classes of human lymphocytes from hematopoietic stem cells (HSCs) will provide new insight into the mechanism of human lymphopoiesis. We report ontogenic, functional, and histologic examination results of reconstituted human lymphocytes in NOD/SCID/γ_c^{null} mice after the transplantation of human cord blood (CB) CD34$^+$ cells. After transplantation, human B, natural killer (NK), and T cells were invariably identified in these mice, even though no human tissues were cotransplanted. Immature B cells resided mainly in bone marrow (BM), whereas mature B cells with surface immunoglobulins were preferentially found in spleen. NK cells were identified in BM and spleen. T cells were observed in various lymphoid organs, but serial examinations after transplantation confirmed human T lymphopoiesis occurring in the thymus. These human lymphocytes were also functionally competent. Human immunoglobulin M (IgM), IgA, and IgG were detected in the sera of these mice. T cells showed a diverse repertoire of T-cell–receptor Vβ (TCR Vβ) chains, proliferated in response to phytohemagglutinin, and were cytotoxic against cell lines. NK activity was demonstrated using the K562 cell line. Immunohistochemical analysis revealed that human lymphocytes formed organized structures in spleen and thymus that were analogous to those seen in humans. In the thymus, CD4 and CD8 double-positive T cells were predominant and coexpressed CD1a and Ki-67, thereby supporting the notion that T lymphopoiesis was taking place. NOD/SCID/γ_c^{null} mice provide a unique model to investigate human lymphopoiesis without the cotransplantation of human tissues. (Blood. 2003;102:873-880)

Introduction

Reconstitution of functional human lymphocytes in experimental animals has been intensely explored because this approach could provide a valuable means of assessing human immunity or of preclinical testing of vaccines, pathogens, and new therapeutic strategies. In 1988, the first reports on engraftment of human hematopoietic cells in homozygous severe combined immunodeficiency disease (*scid*) mice were published.[1,2] McCune et al[1] reported that the simultaneous transplantation of fetal liver hematopoietic cells, fetal thymus, and fetal lymph node resulted in the differentiation of mature human T and B cells (SCID-hu mice model). Mosier et al[2] reported that the transplantation of human peripheral blood (PB) mononuclear cells into *scid* mice resulted in the successful transfer of a functional human immune system (hu-PBL-SCID mice model). These initial models were soon followed by experimental human bone marrow (BM) transplantation into *scid* mice models,[3-9] with modification—the cotransplantation of other human tissues, such as bone, or treating recipient mice with a combination of human cytokines. These modified models showed the multilineage differentiation of human hematopoietic cells to varying degrees. In some experimental settings, SCID-hu mice generated all classes of human immunoglobulins, thereby indicating the presence of human lymphocytes that interacted in response to environmental antigens and that induced B cells to undergo immunoglobulin switching. Although the use of these systems is feasible, they require various kinds of fetal human tissues or human cytokines. Moreover, the procedure is laborious, and engraftment of human hematopoietic cells is highly variable.

To overcome these problems, systematic approaches have been explored. One major approach involves suppressing the innate immunity of *scid* mice, based on the hypothesis that an efficient engraftment level can be achieved by eliminating residual innate immunity in the host. The NOD/SCID mouse strain was found to be an efficient recipient for the reconstitution of human hematopoietic cells.[10-13] However, complete multilineage differentiation, including T cells, has not been achieved using this strain. To suppress residual natural killer (NK) activity in recipient mice, the β2 microglobulin-null ($\beta2m^{-/-}$) allele was backcrossed onto the NOD/LtSz-*scid* background, and a new strain of NOD/SCID-$\beta2m^{null}$ mice was established. In these mice there was an efficient engraftment for human hematopoietic stem cells (HSCs),[14,15] but human T cells were not detected. To improve engraftment efficiency, we established a strain of NOD/Shi-*scid* mice that have a defective common cytokine receptor, γ_c (NOD/SCID/γ_c^{null}).[16] Mutation in the common cytokine receptor γ chain led to a life-threatening, X-linked, severe combined immunodeficiency disease (XSCID) in humans, characterized by an extremely low

From the Department of Pediatrics, Graduate School of Medicine, Kyoto University; and the Central Institute for Experimental Animals, Kawasaki, Japan.

Submitted September 9, 2002; accepted March 13, 2003. Prepublished online as *Blood* First Edition Paper, April 10, 2003; DOI 10.1182/blood-2002-09-2755.

Supported by the Program for the Promotion of Fundamental Studies in Health Science of the Organization for Pharmaceutical Safety and Research of Japan and by a Grant-in-Aid (13GS0009) for Creative Scientific Research, from the Ministry of Education, Science, Technology, Sports and Culture of Japan.

H.H. and R.N. contributed equally to this work.

Reprints: Tatsutoshi Nakahata, Department of Pediatrics, Graduate School of Medicine, Kyoto University, 54 Kawaharacho, Shogoin, Sakyo-ku, Kyoto 606-8507, Japan; e-mail: tnakaha@kuhp.kyoto-u.ac.jp.

The publication costs of this article were defrayed in part by page charge payment. Therefore, and solely to indicate this fact, this article is hereby marked "advertisement" in accordance with 18 U.S.C. section 1734.

number of T and NK cells.[17,18] We observed that NOD/SCID/γ_c^{null} mice had no lymphocytes, no NK activity, and impaired dendritic cell function, thought to lead to high engraftment efficiency and full-lineage differentiation, including those of T cells.[16] Following reports of the generation of functional T cells in these mice,[19] we describe here the results of a comprehensive analysis of human T, B, and NK cells generated in NOD/SCID/γ_c^{null} mice, with regard to developmental process and functional maturation. Human T cells developed in the thymi of these mice, moved to the periphery, and functionally matured to produce cytokines and to have cytotoxicity. Human B cells matured to produce not only human IgM but also IgG and IgA. As in T cells, NK cells matured and had cytotoxicity against K562 cells. Histologic examinations revealed the formation of organized structures of lymphoid organs. This new mouse model is expected to pave the way toward the reconstitution of a human immune system within the body of a laboratory animal.

Materials and methods

Mice

NOD/Shi-*scid*, NOD/SCIDβ2m^{null}, and NOD/SCID/γ_c^{null} mice were used in this study. The NOD/Shi-*scid* strain was established, as reported.[20] NOD/SCID-β2m^{null} mice were purchased from The Jackson Laboratory (Bar Harbor, ME). NOD/SCID/γ_c^{null} mice were developed at the Central Institute of Experimental Animals (Kawasaki, Japan) by crossing NOD/Shi-*scid* mice with C57B6/J-IL-2Rγ^{null} mice. All mice were bred as a homozygous line, shipped to the animal facility of Kyoto University (Kyoto, Japan), and kept under specific pathogen-free conditions in accordance with the guidelines of the facility.

Purification of cell populations

Human CB was collected during normal full-term deliveries, after obtaining informed consent. Mononuclear cells (MNCs) were separated by Ficoll-Hypaque density gradient centrifugation after the depletion of phagocytes with Silica (Immuno Biological Laboratories, Fujioka, Japan). CD34$^+$ cell fractions were isolated using AutoMACS (Miltenyi Biotec GmbH, Bergisch Gladbach, Germany) according to the manufacturer's protocol. Purity was evaluated using flow cytometry. By using Silica and AutoMACS with the most sensitive "Possel d2" protocol, no less than 95% (typically 98%) of the positively selected cells were CD34$^+$. In experiments using lineage-depleted CD34$^+$ cells (Lin$^-$ CD34$^+$), CB MNCs were depleted of lineage-positive cells using StemSep (Stem Cell Technologies, Vancouver, BC, Canada) followed by CD34$^+$ selection with AutoMACS. StemSep contains a cocktail of monoclonal antibodies of antihuman CD2, CD3, CD14, CD16, CD19, CD24, CD56, CD66b, and antihuman glycophorin A. After combined cell selection with StemSep and AutoMACS, almost all the lineage-positive cell fraction was removed. Depletion of CD56$^+$ cells was carried out with AutoMACS and CD56 microbeads (Miltenyi) according to manufacturer's protocol. By choosing the "deplete 025" protocol, almost all CD56$^+$ cells were successfully eliminated.

Transplantation of CB CD34$^+$ cells into mice

Xenotransplantation of purified CB CD34$^+$ cells was performed using a modification of a previously reported method.[11,12] Briefly, 8- to 12-week-old NOD/Shi-*scid*, NOD/SCID-β2m^{null}, and NOD/SCID/γ_c^{null} mice received 240 cGy radiation. The indicated dose of CB CD34$^+$ cells was injected through the tail vein. Only NOD/Shi-*scid* mice were treated with 400 μL phosphate-buffered saline (PBS) containing 20 μL antiasialo GM1 antiserum (Wako, Osaka, Japan) shortly before cell transplantation and every 11th day thereafter. After transplantation, mice were prophylactically provided sterile water with added neomycin sulfate (Gibco BRL, Grand Island, NY).

Flow cytometric analysis of mice with transplanted human cells

PB was taken from the retro-orbital venous plexus at the indicated times after transplantation. Blood was collected through heparinized calibrated pipettes and transferred to EDTA (ethylenediaminetetraacetic acid)–2 Na containing CAPIJECT (Terumo Medical, Somerset, NJ). Lineage analysis of human hematopoietic cells was made using flow cytometry (FACScalibur; BD PharMingen, San Diego, CA) according to the manufacturer's protocol. Mice were killed by cervical dislocation more than 5 months after cell transplantation. BM, spleens, and thymi were analyzed using flow cytometry. Antibodies used for flow cytometric analysis were antihuman CD45-fluorescein isothiocyanate (CD45-FITC), CD3-FITC, TdT-FITC, CD34-phycoerythrin (CD34-PE), CD10-PE, CD3-PE, T-cell receptor (TCR) γδ-PE, CD158a-PE, KIR p70-PE, antihuman surface IgD-PE, IgM-PE, IgG-PE, IgA-PE, CD8-phycoerythrin 5-succinimidylester (PC5), CD19-PC5, TCR αβ-PC5, and antimouse CD45-allophycocyanin (CD45-APC). Antibodies conjugated with FITC, PE, or APC were purchased from BD PharMingen except anti–CD158a-PE and anti–KIR p70-PE. Antibodies conjugated with PC5, anti-CD158a-PE, and anti-KIR p70-PE were purchased from Immunotech (Marseilles, France). The Vβ repertoire of TCR was analyzed using IOTest Beta Mark TCRVβ Repertoire kits (Immunotech).

Reverse transcription–polymerase chain reaction

RNA was isolated from the spleen and BM of NOD/SCID/γ_c^{null} mice with or without transplanted CD34$^+$ cell using TRIzol Reagent (Invitrogen, Carlsbad, CA). Total RNA (1 μg) was taken from each sample and subjected to reverse transcription using SuperScript (Invitrogen). Using one-twentieth synthesized cDNA, PCR amplification was carried out with Takara LA Taq (Takara Bio, Ohtsu, Japan). Samples were denatured at 94°C for 5 minutes, then amplified by rounds consisting of 94°C for 30 seconds (denaturing), 60°C for 30 seconds (annealing), and 72°C for 30 seconds (extension) for 31 cycles using primer sets as follows: interleukin-2 (IL-2), 5′-CTTCAGTGTCTAGAAGAAGAACTCAA-3′ and 5′-GGTAAACCATTTTAGAGCCCC-3′; IL-15, 5′-CTGACTCTCAGTTCAGTTTTACTCT-3′ and 5′-TCTAAGCAGCAGAGTGATGTTTG-3′; human hypoxanthine phosphoribosyltransferase (HPRT) 5′-AATTATGGACAGGACTGAACGTC-3′ and 5′-CGTGGGGTCCTTTTCACCAGCAAG-3′; mouse HPRT 5′-GCTGGTGAAAAGGACCTCT-3′ and 5′-CACAGGACTAGAACACCTGC-3′. PCR products were separated on 2.0% agarose gel, stained with ethidium bromide, and photographed.

Functional analysis of human lymphocytes generated in NOD/SCID/γ_c^{null} mice

Anti–CD3-dependent cytotoxic T lymphocyte (CTL) activity was tested using a calcine release assay, with minor modification.[21] Briefly, human MNCs in the spleen of a mouse that underwent cell transplantation were separated by Ficoll-Hypaque density gradient centrifugation. MNCs were cultured at 1 × 10^6/mL in RPMI 1640 supplemented with 10% fetal bovine serum (FBS) with phytohemagglutinin (PHA; 1 μg/mL) and human IL-2 (50 IU/mL) for 48 hours. After taking the supernatant to analyze human cytokine production, culture was continued without PHA for 8 additional days. Expanded lymphocytes were suspended in Hanks balanced salt solution supplemented with 5% FBS. Target cells labeled with calcine-AM (Molecular Probes, Eugene, OR) were mixed with T blasts at the indicated effector-target (E/T) ratios in the presence of anti-CD3 monoclonal antibody (mAb). Cells with isotype-control mAb or without mAb were also prepared as negative controls. After 3 hours of incubation, the release of calcine into the supernatant was measured with an automated fluorescence scanner (Wallac 1420ARVOsx; Perkin Elmer, Fremont, CA). NK cell activity was measured in a similar way. In analyzing NK cell activity, expanded lymphocytes were mixed with calcine-labeled K562 cells without antibodies. The CD56$^+$ NK cell population comprised less than 10% expanded lymphocytes. To measure the total release of calcine, 100 μL lysis buffer (50 mM sodium-borate, 0.1% Triton X-100, pH 9.0) was added to the wells with only labeled target cells after aliquots of supernatant had been taken to measure spontaneous release. Percentage cytotoxicity was determined using the following equation: (F CTL assay − F spontaneous

release)/(*F* total lysis − *F* spontaneous release) × 100 = % cytotoxicity, where *F* represents fluorescence. All assays were performed in quadruplicate, and PB MNCs of a healthy adult donor served as a positive control. Human cytokine analysis was made using the Cytometric Bead Array Kit for human cytokines according to the manufacturer's protocol (BD PharMingen). Intracellular cytokine staining was performed as follows: PHA-stimulated splenocytes were further stimulated with 10 ng/mL phorbol ester (PMA; Sigma, St Louis, MO) and 1 μg/mL Ca^{2+} ionophore (ionomycin; Sigma) for 6 hours. Brefeldin A (Sigma) was added at final concentration of 10 μg/mL during the last 2 hours. Cells were washed with PBS with 2% FCS and stained with antihuman CD56-PC5 (Immunotech). Then the cells were washed with PBS with 2% FCS, fixed, and permeabilized with Cytofix/Cytoperm (BD PharMingen) for 20 minutes. After washing with Perm/Wash (BD PharMingen) twice, the cells were incubated with FITC- or PE-conjugated isotype control mAb (BD PharMingen), anti–IFN-γ (BD PharMingen), anti–IL-4 (BD PharMingen), and anti–tumor necrosis factor-α (anti–TNF-α) (Immunotech) for 30 minutes at 4°C. After washing with Perm/Wash, the cells were analyzed by flow cytometry.

Immunoglobulin analysis

Human IgA, IgM, and IgG in plasma of NOD/SCID/γ_c^{null} or NOD/SCID-$\beta 2m^{null}$ mice were measured using human immunoglobulin assay kits (Bethyl, Montgomery, TX). Cross-reactivity against mouse IgG, IgA, and IgM checked with mouse serum standard (Bethyl) were 0.1% for IgM and less than 0.01% for IgG and IgM.

Immunohistochemical and immunofluorescence analysis

Frozen blocks were cut at 4 to 6 μm, and, after air-drying, sections were fixed in cold acetone. After blocking with 0.5% casein and 5% goat serum, the following primary antibodies were incubated for 1 hour at room temperature: mouse antihuman CD3 (UCHT-1), mouse antihuman CD20-EPOS (2L6), mouse antihuman CD1a (BL6), and mouse antihuman Ki-67 (MIB-1). An appropriate secondary antibody was incubated for 30 minutes, and either DAB or VECTOR Blue (Vector Laboratories, Burlingame, CA) was used for visualization. For confocal microscopy, each tissue was stained sequentially with mouse antihuman CD4 (NU-$T_{H/I}$) followed by a Cy3-labeled F(ab')$_2$ fragment of donkey antimouse IgG and with biotinylated mouse antihuman CD8 (HIT8α) followed by streptavidin Alexa 488.

Statistical analysis

Data are presented as the mean ± SEM. Statistical significance was determined using the Mann-Whitney *U* test. $P < .05$.

Results

Efficient engraftment and full lineage lymphoid differentiation from CB CD34$^+$ cells in NOD/SCID/γ_c^{null} mice

To evaluate the efficiency of engraftment of human hematopoietic cells in NOD/SCID/γ_c^{null} mice, 1×10^4 or 5×10^4 CB CD34$^+$ cells were transplanted into NOD/SCID/γ_c^{null} mice, and 1×10^5 CB CD34$^+$ cells were transplanted into NOD/Shi-*scid* (NOD/SCID) mice; the engrafted human hematopoietic cells were then analyzed using flow cytometry. Three months after transplantation, the percentage of human CD45$^+$ cells in the peripheral blood was much higher in NOD/SCID/γ_c^{null} mice, even though the transplanted cell dose was only one half or one tenth that for NOD/SCID mice (Figure 1A). Four months after transplantation of 1×10^5 CB CD34$^+$ cells, the percentage of human CD45$^+$ cells in the BM of NOD/SCID/γ_c^{null} mice was much higher than that in NOD/SCID (72.6% ± 6.3% vs 10.6% ± 4.4%; n = 8; $P < .01$).[16]

Analysis of BM and spleen revealed that the NOD/SCID/γ_c^{null} mice carried all classes of human lymphocytes—human CD3$^+$ T cells, CD3$^-$CD56$^+$ NK cells, and CD19$^+$ B cells. CD5$^+$ B cells were considered to constitute an ontogenically unique subpopulation (Figure 1B). Expression of killer inhibitory receptor (KIR) antigens, such as CD158a and KIR p70, was also identified on a population of CD56$^+$ NK cells (Figure 1C). Human B cells and NK cells were detected in NOD/SCID mice, but the percentage of these cells was low and human CD3$^+$ T cells were never identified.

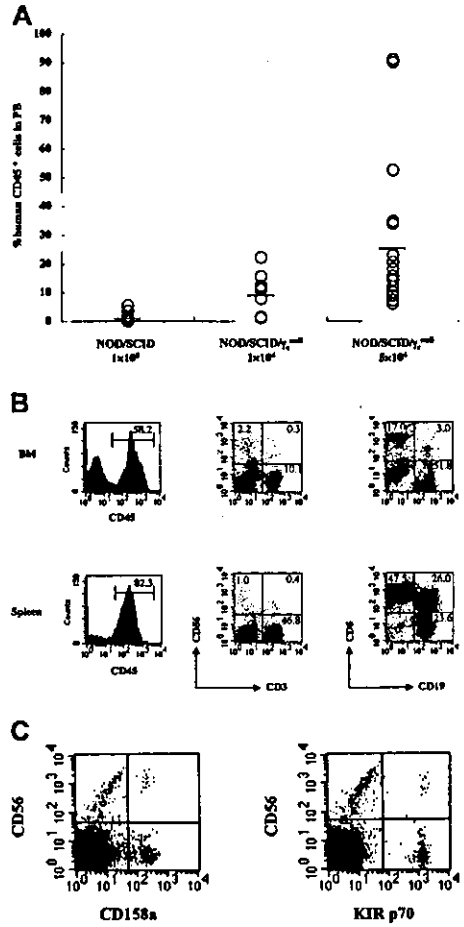

Figure 1. Efficient engraftment and complete reconstitution of human lymphocytes in NOD/SCID/γ_c^{null} mice that underwent transplantation with CB CD34$^+$ cells. 1×10^4 (n = 7) or 5×10^4 (n = 17) CB CD34$^+$ cells were transplanted into NOD/SCID/γ_c^{null} mice, and 1×10^5 (n = 15) CB CD34$^+$ cells were transplanted into NOD/SCID mice. (A) Percentages of human CD45$^+$ cells in PB of mice were analyzed 3 months after transplantation using flow cytometry. Percentages of human CD45$^+$ cells were calculated as: % human CD45$^+$ = human CD45$^+$ cells/(human CD45$^+$ cells + mouse CD45$^+$ cells) × 100. Results of 7 independent experiments are shown. (B) Representative FACS analysis of human lymphocytes in BM and spleen of NOD/SCID/γ_c^{null} mice that underwent transplantation with CB CD34$^+$ cells. (C) Representative FACS analysis of KIR antigens is shown. CD158a or KIR p70 were detected on 7.7% or 3.8% of CD56$^+$ cells, respectively.

Flow cytometric analysis of human T cells in NOD/SCID/γ_c^{null} mice after transplantation of CB CD34$^+$ cells

Next, we focused on human T cells in the NOD/SCID/γ_c^{null} mice. After the transplantation of 4×10^4 CB CD34$^+$ cells into NOD/SCID/γ_c^{null}, NOD/SCID-$\beta 2m^{null}$, and NOD/SCID mice, human CD3$^+$ T cells in PB were measured sequentially using flow cytometry. Human T cells were identified only in NOD/SCID/γ_c^{null} mice, and the percentage of T cells was gradually increased with time (Figure 2A).

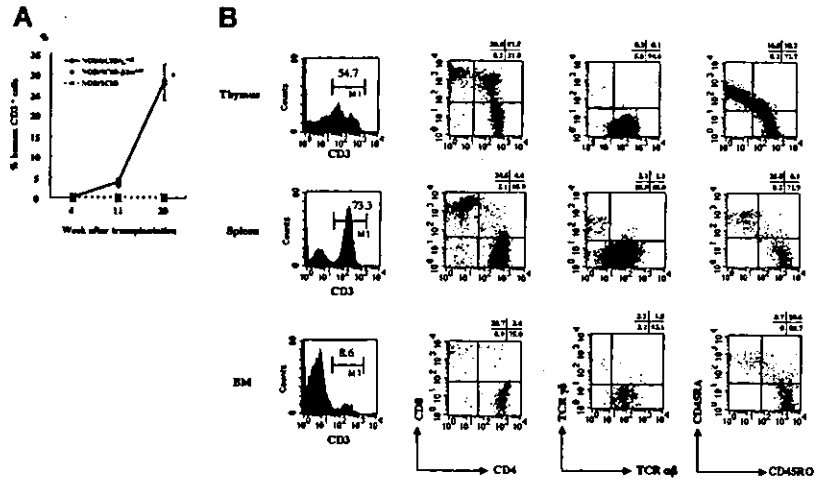

Figure 2. Human CD3⁺ cells in PB of NOD/SCID/γ_c^{null}, NOD/SCID-β2m^{null}, and NOD/SCID mice that underwent transplantation with CB CD34⁺ cells. (A) Percentage of human CD3⁺ cells among human CD45⁺ cells in PB was analyzed sequentially after the transplantation of 4×10^4 CB CD34⁺ cells. Results of 2 independent experiments (n = 3 each) are shown. Error bars represent SDs. (B) Surface phenotypes of human CD3⁺ T cells in thymus, spleen, and BM of NOD/SCID/γ_c^{null} mice were evaluated 5 months after the transplantation of 2 to 4×10^4 CB CD34⁺ cells. Representative data from 5 independent analyses of similar results are shown.

The surface phenotype of human T cells in the thymus, spleen, and BM was analyzed 5 months after transplantation using flow cytometry (Figure 2B). The thymi were always highly atrophic at this time, and approximately 2 to 5×10^5 human nucleated cells were identified.

Two subpopulations of CD3⁺ T cells, CD3^{high} and CD3^{low}, were identified in the thymus, but almost all the T cells in the spleen and BM had the CD3^{high} phenotype. Simultaneous staining of CD4 and CD8 revealed that CD4⁺CD8⁺ double-positive (DP) T cells were predominant in the thymus, whereas CD4⁺ or CD8⁺ single-positive (SP) T cells were predominant in the spleen and BM. Analysis of the TCR revealed that almost all T cells had αβ TCR in the thymus but that T cells with γδ TCR were also detected in the spleen and BM. Considerable numbers of naive T cells of the CD3⁺CD45RA⁺ phenotype were identified in all organs analyzed. NOD/SCID/γ_c^{null} mice with transplanted CB CD34⁺ cells showed little clinical evidence of graft-versus-host disease (GVHD), whereas transplantation of PB CD3⁺ cells evoked GVHD responses even shortly after the procedure (data not shown). Transplantation of CB CD3⁺CD45RA⁺ cells did not result in the maintenance of human T cells for more than 3 months (data not shown). These results are highly suggestive of the de novo generation of human T cells from HSCs in these mice.

Development of human T cells in the thymi of NOD/SCID/γ_c^{null} mice

To confirm the de novo generation of human T cells from HSCs and to clarify the site(s) responsible, we transplanted further purified lineage-depleted (Lin⁻) CB CD34⁺ cells into NOD/SCID/γ_c^{null} mice. The purity of transplanted Lin⁻ CD34⁺ was greater than 98%, and contamination of CD3⁺ cells was not identified by flow cytometry (Figure 3A). After the transplantation of 5×10^4 Lin⁻ CD34⁺ cells, various organs were analyzed through flow cytometry (Figure 3B-C).

After the transplantation of CB Lin⁻ CD34⁺ or CB CD34⁺ cells, human T cells became detectable in PB at approximately the 8th week. Therefore, we conducted our analysis shortly before (6th week after transplantation) and after (9th week after transplantation) the emergence of human T cells. At the 6th week, T cells were identified in the thymus, yet spleen, BM, and liver had no T cells. T cells in the thymus consisted mainly of DP T cells with barely detectable levels of double-negative (DN) T cells. At the 9th week, the thymus was further engrafted with DP T cells, and the spleen began to show a small number of T cells with the SP phenotype. These results clearly indicated that de novo generation of human T cells occurred in the thymus of NOD/SCID/γ_c^{null} mice, followed by seeding of these cells in peripheral organs such as the spleen.

Human B-cell development and immunoglobulin production in NOD/SCID/γ_c^{null} mice

B-cell–specific markers of human hematopoietic cells in the BM and spleen of NOD/SCID/γ_c^{null} mice were evaluated using flow cytometry (Figure 4A). In the BM, phenotypically immature B cells were predominant. A large number of human CD19⁺ B cells simultaneously expressed human CD34 or CD10. Terminal deoxytransferase (TdT)⁺ B cells were also identified in BM and corresponded to premature pro-B cells. Human surface immunoglobulin expression showed immature B cells (IgM⁺) to be the major population. On the other hand, most human B cells in the spleen were mature. The expression of human CD34 or TdT was hardly detectable, and human surface IgM⁺ and IgD⁺ B cells were more abundant than in the BM. To determine whether these B cells were functionally mature, we measured plasma human immunoglobulin levels using enzyme-linked immunosorbent assay (ELISA) (Figure 4B).

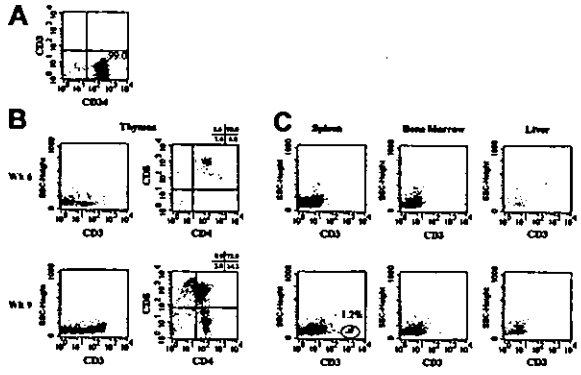

Figure 3. Human T cells in various organs of NOD/SCID/γ_c^{null} mice that underwent transplantation with CB Lin⁻ CD34⁺ cells. Human CD3⁺ cells in thymus, spleen, bone marrow, and liver were analyzed using flow cytometry at 6 and 9 weeks after the transplantation of 5×10^4 CB Lin⁻ CD34⁺ cells. (A) The purity of Lin⁻ CD34⁺ cells was evaluated using flow cytometry. (B) Expressions of human CD3, CD4, and CD8 on human CD45⁺ cells in thymus are shown. (C) Expressions of human CD3 on human CD45⁺ cells in spleen, bone marrow, and liver are shown.

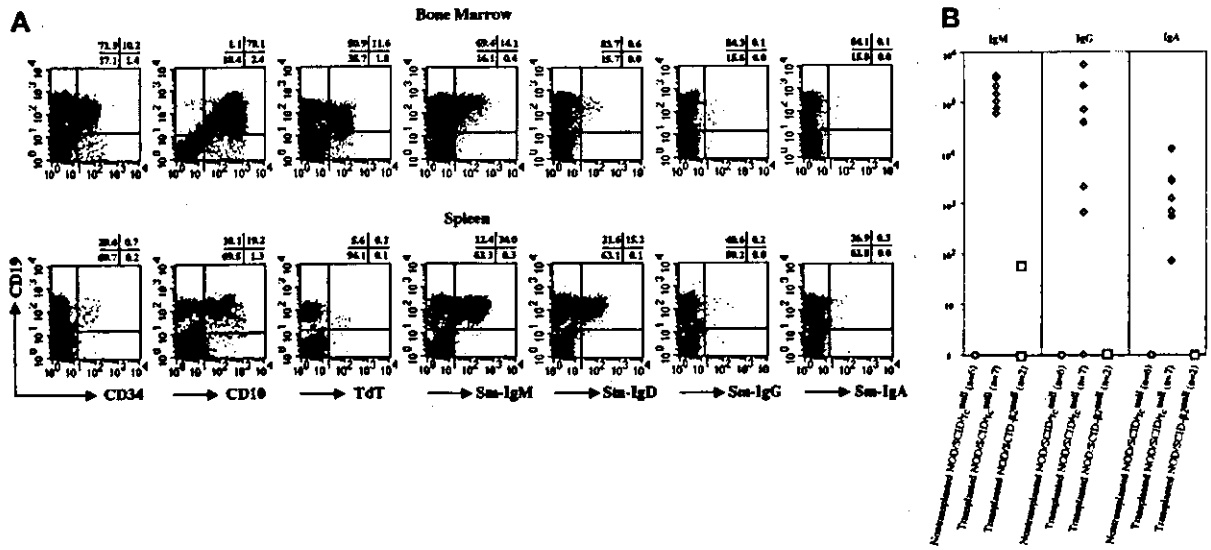

Figure 4. B-cell development in NOD/SCID/γ_c^{null} mice that underwent transplantation with CB CD34$^+$ cells. (A) Surface expressions of CD34, CD10, CD19, IgM, IgD, IgG, and IgA and intracellular expression of TdT were examined after setting a gate on the human CD45$^+$ population. (B) Human IgM, IgG, and IgA concentrations in plasma of NOD/SCID/γ_c^{null} and NOD/SCID-$\beta2m^{null}$ mice that underwent transplantation with 4 × 10^4 CB CD34$^+$ cells were measured by ELISA.

All NOD/SCID/γ_c^{null} mice that underwent CB CD34$^+$ cell transplantation produced not only human IgM but also IgG and IgA. For comparative purposes, NOD/SCID-$\beta2m^{null}$ mice, which were reported to be better recipients for human HSCs,[14] were also evaluated for the production of human immunoglobulin after transplantation with 4 × 10^4 CB CD34$^+$ cells. Only one NOD/SCID-$\beta2m^{null}$ mouse had very low levels of IgM, and other types of immunoglobulin were not detected. Thus, the differentiation of B cells occurred mainly in the BM of NOD/SCID/γ_c^{null} mice then functionally maturated to produce human immunoglobulin with isotype switching from IgM to IgG and IgA.

Diverse Vβ repertoire of human T cells undergoing differentiation in NOD/SCID/γ_c^{null} mice

To determine whether the differentiation of human T cells in NOD/SCID/γ_c^{null} mice proceeded in a coordinated manner, recombination diversity of TCR was analyzed using flow cytometry. Five to 6 months after the transplantation of CB CD34$^+$ cells, the TCR repertoire of human T cells in the spleen of NOD/SCID/γ_c^{null} mice was quantified using a panel of 24 different antibodies specific to each Vβ (Figure 5).

Surprisingly, a diverse T-cell repertoire was confirmed in each experiment. These results imply that in the NOD/SCID/γ_c^{null} mice with transplanted CB CD34$^+$ cells, a tightly regulated program of sequential TCR gene expression occurred that altered the phenotypes of developing cells and finally promoted the generation of a diverse Vβ repertoire.

Functional maturation of human T cells and NK cells differentiated in NOD/SCID/γ_c^{null} mice

We further analyzed the functions of human T cells and NK cells developing in NOD/SCID/γ_c^{null} mice. Human mononuclear cells in spleens of mice that underwent transplantation were cultured in the presence of PHA and human IL-2 for 2 days, after which the supernatant was taken to assess human cytokine production. Cultures were continued without PHA for 8 additional days to yield enough cells to evaluate cytotoxicity. Human T cells in NOD/SCID/γ_c^{null} mice responded to the stimulation of PHA and showed characteristics of T-cell blasts. The number of cells expanded more than 10-fold at day 10 (Figure 6A). These data suggest that the signals of PHA were transduced through the TCR of these T cells and resulted in cell expansion. Human interferon-γ (IFN-γ), TNF-α, IL-10, IL-5, and, though barely detectable, IL-4 was also identified in the supernatant of PHA-stimulated T cells (Figure 6B). To investigate the cytokine production of NK cells, we performed intracellular cytokine staining. Considerable populations of CD56$^+$ NK cells produced IFN-γ or TNF-α, and IL-4 production was limited (Figure 6C). Concerning NK cell development, it has been

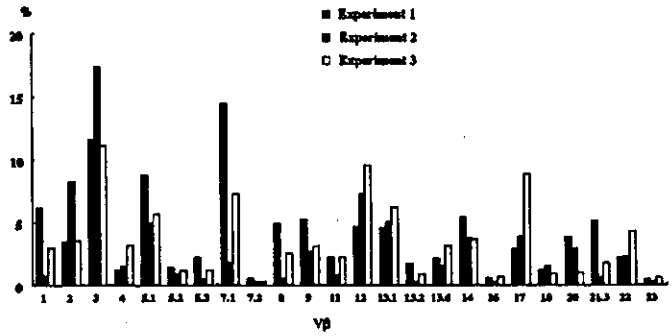

Figure 5. TCR Vβ repertoire analysis of human T cells in spleen. Four to 6 months after the transplantation of 2 × 10^4 to 5 × 10^4 CB CD34$^+$ cells, spleen cells were taken and the TCR Vβ repertoire was analyzed by flow cytometry using a panel of 24 different antibodies. The results of 3 independent experiments are shown.

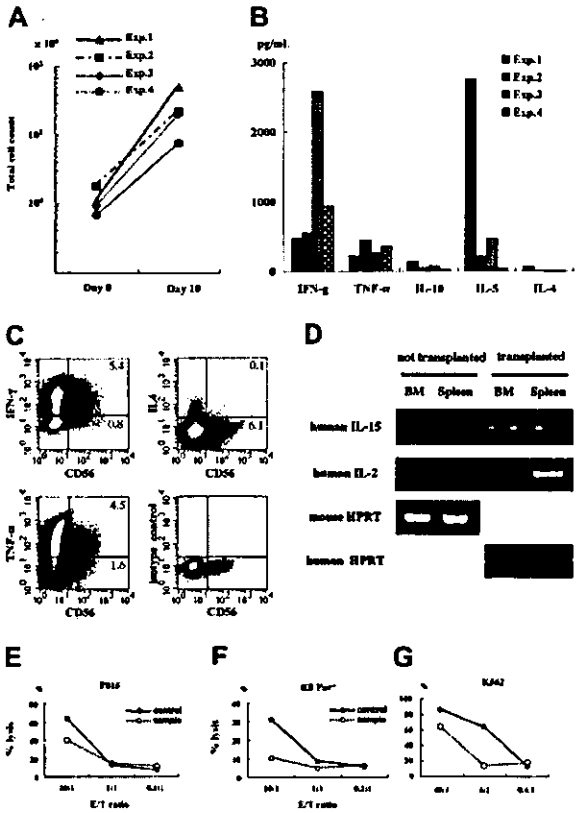

Figure 6. Functional analysis of human lymphocytes in spleen of NOD/SCID/γ_c^{null} mice. Four to 6 months after the transplantation of 2 × 10^4 to 5 × 10^4 CB CD34$^+$ cells, human lymphocytes in spleen were cultured and expanded for functional analyses. (A) Cell proliferation after 10-day culture; PHA (1 μg/mL) and hIL-2 (50 IU/mL) for the initial 48 hours followed by hIL-2 (50 IU/mL) only for 8 days. (B) Supernatants of the spleen cells after 48-hour stimulation with PHA and hIL-2 were taken, and the production of human cytokines was evaluated using Cytometric Bead Array Kit for human cytokine (BD PharMingen). (C) PHA-stimulated human lymphocytes were further stimulated with 10 ng/mL PMA and 1 μg/mL ionomycin for 6 hours. Brefeldin A was added during the last 2 hours. Then the cells were stained with membrane CD56 and intracellular cytokines and were analyzed using flow cytometry. (D) RNA was isolated from the spleen and BM of NOD/SCID/γ_c^{null} mice with or without transplanted CD34$^+$ cells, and the expression of mRNA for human IL-2 and IL-15 was examined by RT-PCR. Human or mouse HPRT was used as a positive control. (E-G) Anti–CD3-dependent cytotoxic T-lymphocyte activity and NK activity were evaluated by measuring the release of calcine-AM into the supernatant after cytolysis of target cells labeled with calcine. Results are expressed as the percentage of specific lysis. PB MNCs of a healthy adult were used as a positive control. Representative data with similar results of 4 independent experiments are shown.

reported that IL-2 and IL-15 are essential to the development and maintenance of NK cells.[22,23] Therefore, we also examined the production of these cytokines by reverse transcription–polymerase chain reaction (RT-PCR) and identified them in the spleen and BM of NOD/SCID/γ_c^{null} mice with transplanted CD34$^+$ (Figure 6D).

Further, these T cells exerted cell-mediated cytotoxicity. Fas + perforin-dependent or perforin-dependent cytotoxicity was evaluated using P815 cells or the Fas-deficient Epstein-Barr virus–transformed B-cell line ($Fas^{-/-}$ EB) as target cells, respectively. Fas + perforin-dependent cytotoxicity was comparable but a little lower than in a healthy adult human (Figure 6E). Cytotoxic activity dependent solely on the perforin-mediated pathway was lower than in control (Figure 6F). Although the value was not enough to be statistically significant, the percentage lysis of $Fas^{-/-}$ EB cells by samples always surpassed those of negative controls (typically less than 5% and never more than 10%), which are the ones with isotype control mAb or without antibody. Further investigation will be needed to clarify the pathway involved in the killing by these cells. Natural killer activity was evaluated using K562 cells, which are commonly used for the assessment of NK cell activity.[24] As shown in Figure 6G, human mononuclear cells in the spleens of NOD/SCID/γ_c^{null} mice showed substantial levels of cytotoxicity against K562 cells, suggesting that human NK cells functionally matured. However, to exclude the possibility that coexisting other cells, such as T cells in the test sample, might contribute to K562 cell killing, we performed the same experiments with human CD56-depleted splenocytes as effector cells. Human CD56 depletion abrogated K562 cell killing almost completely (99.8% ± 0.03% inhibition; n = 3), which clearly demonstrated that the lysis of K562 cells was attributable to NK cells.

Histologic evaluation of reconstituted lymphoid organs

Lymphoid organs in NOD/SCID/γ_c^{null} mice that received transplanted human CD34$^+$ CB cells were examined histologically 5 months after transplantation (Figure 7). Although the thymus of the recipient mouse was highly atrophic, human CD45$^+$ cells were identified, usually as CD3$^+$ T cells. These T cells were predominantly CD4$^+$CD8$^+$ DP T cells and were positive for human CD1a$^+$, which is expressed on immature thymocytes. These cells were also positive for the cell-cycle–specific antigen Ki-67. Cytokeratin staining revealed the presence of an epithelial cell network inside the thymus, and these epithelial cells were positive for major histocompatibility complex class 2 (MHC class 2) of NOD mice (data not shown). These findings suggested that the immature human T cells that resided in the epithelial network were of mouse origin. In the spleen, a mononuclear cell-rich region similar to

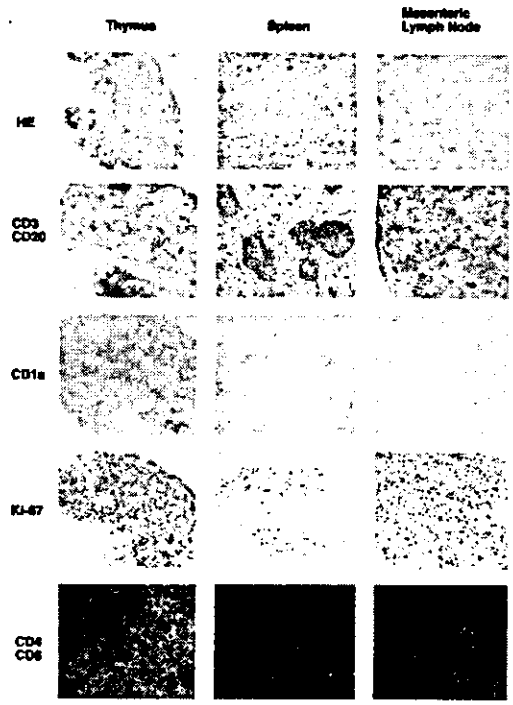

Figure 7. Immunohistochemical staining of the thymus, spleen, and mesenteric lymph nodes. Six months after transplantation, various organs were taken, and frozen sections were prepared. Expressions of human CD3 (Vector Blue)/human CD20 (DAB), human CD1a (Vector Blue), human Ki-67 (Vector Blue), and human CD4 (Alexa 488)/human CD8 (Cy3) were evaluated. Original magnification is × 400 for CD4/CD8 images, × 100 for all others.

white pulp appeared after transplantation. This structure was never found in NOD/SCID/γ_c^{null} mice that did not undergo transplantation. Antihuman CD45 staining showed that the cell-rich region consisted mainly of human hematopoietic cells. Antihuman CD3 and CD20 double staining revealed that the structure consisted of human CD3$^+$ cells surrounding a vessel and human CD20$^+$ cells flanking the CD3$^+$-cell–rich region. This structure resembled a periarteriolar lymphoid sheath (PALS) and primary follicles seen in humans. Mesenteric lymph nodes in NOD/SCID/γ_c^{null} mice with transplanted CB CD34$^+$ cells also consisted mainly of human CD3$^+$ cells. Double staining with CD3 and CD20 revealed that this tissue was densely engrafted with human T and B cells but devoid of typical follicular structures. These findings indicated that organized structures of the thymus, spleen, and mesenteric lymph nodes were reconstituted to a considerable extent by human-derived lymphocytes in NOD/SCIDγ_c^{null} mice.

Discussion

Development and functional maturation of human lymphocytes are achieved through complex networks in various organs, such as BM, thymus, spleen, and lymph node. Many attempts have been made to reconstitute a functional human immune system in mice with the *scid* phenotype but have resulted in limited success.[1-3,25-27] We obtained evidence for the reconstitution of functional T cells, B cells, and NK cells from CB CD34$^+$ cells in NOD/SCID/γ_c^{null} mice without the cotransplantation of human tissues. After the transplantation of CB CD34$^+$ cells, all classes of human lymphocytes were invariably identified. T-cell development and maturation levels in these mice were similar to those in humans. The thymus contained immature T cells of DP and DN phenotypes, and the spleen was rich in mature SP T cells. CD3$^+$CD45$^+$ naive T cells were generated to an extent comparable to that in humans. The TCR of these T cells was predominantly $\alpha\beta$, but T cells with $\gamma\delta$TCR were also observed in the spleen. Flow-cytometry–based quantification of TCR Vβ (TCRBV) of human CD3$^+$ cells in the spleen showed a divergent repertoire, thus implying acquisition of the potential to respond to highly diverse molecules. Indeed, generated T cells proliferated with PHA stimulation and produced human cytokines. These T blasts showed cell-mediated cytotoxicity, thereby demonstrating the functional maturation of human T cells in a mouse environment. Like T cells, NK cells were mature enough to exert cytotoxicity against K562 cells. B-cell development and maturation levels were also comparable to those in humans. Immature B cells predominantly resided in the BM, and mature surface immunoglobulin-positive B cells were predominant in the spleen. Although human B-cell differentiation can be seen in NOD/SCID mice, only the NOD/SCID/γ_c^{null} mice model enabled human IgM, IgG, and IgA production in mouse serum, which means that the generated human T and B cells were functionally competent. These findings suggest that complicated developmental processes of T and B lymphocytes were reproduced in the NOD/SCID/γ_c^{null} mice model.

In the SCID-hu mouse model, simultaneous implantation of fetal thymus and liver was indispensable for the generation of functionally mature human T cells.[8] In the beige/nude/xid/human (bnx/hu) mice model, human T cells could develop from HSCs through the cotransplantation of genetically altered human BM stromal cells, which produced human cytokines.[28] However, extrathymically developed T cells were functionally impaired. Systemic administration of human IL-7 restored function, but to a limited extent.[9] Considering these findings, NOD/SCID/γ_c^{null} mice seemed to provide an excellent environment for human T-cell development. Contrary to previous models, the NOD/SCID/γ_c^{null} mice model did not require the cotransplantation of human tissue. The interesting question is whether these mice have unique properties for human lymphocyte development or a profound immunodeficiency that enables some kind of human tissue formation. Production of IL-2 and IL-15, which are essential for NK cell development, in these mice after transplantation may suggest that this model can reconstitute the environment required for lymphopoiesis. More detailed identification of engrafted human cells is under investigation. Organized clustering of lymphocytes in appropriate organs is required for the reconstitution of a functional immune system. In NOD/SCID/γ_c^{null} mice with transplanted human CB CD34$^+$ cells, T- and B-cell clustering is seen in the thymus, spleen, and lymph nodes. The thymus was engrafted with immature T cells, whereas the spleen contained mature T cells that formed clusters with B cells. PALS-like structures consisting mainly of human hematopoietic cells were also identified, and these structures were absent before transplantation. In lymph nodes, many T and B cells were identified, but distinct follicular structures were missing. This may reflect that critical molecules for lymphocytes, such as adhesion molecules or chemokines, are not available for human cells in a mouse environment, which could prove an obstacle to analyzing the human immune system in detail.

One important question is how human T cells develop. Human CD3$^+$ T cells with the CD4$^+$CD8$^+$ DP phenotype in the thymus were positive for human CD1a, which is expressed on immature thymocytes.[29] These cells were also positive for TdT (data not shown) and the cell-cycle–specific antigen Ki-67. Furthermore, cytokeratin staining revealed the presence of an epithelial cell network derived mainly from mice (data not shown). These results strongly suggest that the generation of human T cells occurs in the thymus of NOD/SCID/γ_c^{null} mice. To exclude the possibility that contaminated T cells expanded in mice, we transplanted CB Lin$^-$ CD34$^+$ cells into NOD/SCID/γ_c^{null} mice and performed sequential analysis. T cells first appeared only in the thymus with the phenotype of immature thymocytes, followed by seeding to peripheral organs. This finding supports the notion that human T cells were derived from HSCs, maturated in the mouse thymus, and seeded to the periphery. Another important observation is that as few as 100 CD34$^+$ cells could engraft and give rise to multilineage blood cells in our mice, as we have already reported.[16] Even after the transplantation of these few CD34$^+$ cells, we confirmed the presence of CD3$^+$ cells 5 months after transplantation using flow cytometry. Although our results strongly suggest the generation of human T cells in the mouse thymus, the possibility of extrathymic differentiation must be examined. To clarify the site(s) for T-cell development, the results of thymectomy experiments have to be analyzed. It is also noteworthy that NOD/SCID/γ_c^{null} mice with transplanted human CB CD34$^+$ cells showed almost no appreciable evidence of GVHD responses despite a considerable number of human T cells in these mice. Transfer of human PB lymphocytes into *scid* mice induces a substantial immune response against mouse xenoantigens that skews the human TCR repertoire[30] and induces GVHD.[31,32] The mice died within a few weeks. Under physiological conditions, intrathymic T-cell differentiation is characterized by 2 selection events: positive and negative selection. Two types of molecules produced by nonlymphoid thymic cells—MHC molecules and cytokines—play important roles in T-cell maturation. MHC molecules are indispensable for positive and negative selection, serving to preserve useful cells and to eliminate potentially harmful ones. As for which MHC restriction orchestrates human lymphocyte development, at least 2 possibilities are

likely. One is human MHC. Sanchez et al[33] reported that human CB contains a cell population that supports the differentiation of $CD34^+$ cells into $CD4^+$ or $CD8^+$ naive T cells in serum-deprived cultures. The other possibility is xenogenic mouse MHC. Robin et al[34] and Weekx et al[35] reported the generation of human T-lymphoid progenitor cells from $CD34^+CD38^-$, $CD34^+CD38^{low}$, and $CD34^+CD38^+$ subsets of human CB and BM cells in fetal thymus organ cultures from NOD/SCID or *scid* mice. Zhao et al[36] also showed that normal immune functions and specific T-cell tolerance to discordant xenogenic donors were achieved by grafting fetal pig thymus and liver tissue to T-cell– and NK-cell–depleted thymectomized mice. These 2 possibilities—human MHC and xenogenic mouse MHC—must be examined further to elucidate the mechanism underlying the generation of human T cells in NOD/SCID/γ_c^{null} mice.

Our mouse model is an excellent in vivo model in which to complete the reconstitution of human lymphocytes from HSCs without transplanting additional human tissues. Use of this model will be a unique way to investigate human lymphopoiesis, which has been analyzed in a combination of different assay systems. We conclude that NOD/SCID/γ_c^{null} mice are a potent and versatile species that can be used to analyze human lymphopoiesis and human HSCs.

Acknowledgments

We thank Dr M. Yasukawa for kindly providing the EB $Fas^{-/-}$cell line, Dr K. Omori (Kyoto University Hospital, Kyoto, Japan) for helpful discussions, and M. Ohara (Fukuoka, Japan) for language assistance.

References

1. McCune JM, Namikawa R, Kaneshima H, Shultz LD, Lieberman M, Weissman IL. The SCID-hu mouse: murine model for the analysis of human hematolymphoid differentiation and function. Science. 1988;241:1632-1639.
2. Mosier DE, Gulizia RJ, Baird SM, Wilson DB. Transfer of a functional human immune system to mice with severe combined immunodeficiency. Nature. 1988;335:256-259.
3. Namikawa R, Weilbaecher KN, Kaneshima H, Yee EJ, McCune JM. Long-term human hematopoiesis in the SCID-hu mouse. J Exp Med. 1990; 172:1055-1063.
4. Lapidot T, Pflumio F, Doedens M, Murdoch B, Williams DE, Dick JE. Cytokine stimulation of multilineage hematopoiesis from immature human cells engrafted in SCID mice. Science. 1992;255: 1137-1141.
5. Kyoizumi S, Baum CM, Kaneshima H, McCune JM, Yee EJ, Namikawa R. Implantation and maintenance of functional human bone marrow in SCID-hu mice. Blood. 1992;79:1704-1711.
6. Carballido JM, Schols D, Namikawa R, et al. IL-4 induces human B cell maturation and IgE synthesis in SCID-hu mice: inhibition of ongoing IgE production by in vivo treatment with an IL-4/IL-13 receptor antagonist. J Immunol. 1995;155:4162-4170.
7. Roncarolo MG, Carballido JM, Rouleau M, Namikawa R, de Vries JE. Human T- and B-cell functions in SCID-hu mice. Semin Immunol. 1996;8: 207-213.
8. Carballido JM, Namikawa R, Carballido-Perrig N, Antonenko S, Roncarolo MG, de Vries JE. Generation of primary antigen-specific human T- and B-cell responses in immunocompetent SCID-hu mice. Nat Med. 2000;6:103-106.
9. Tsark EC, Dao MA, Wang X, Weinberg K, Nolta JA. IL-7 enhances the responsiveness of human T cells that develop in the bone marrow of athymic mice. J Immunol. 2001;166:170-181.
10. Hesselton RM, Greiner DL, Mordes JP, Rajan TV, Sullivan JL, Shultz LD. High levels of human peripheral blood mononuclear cell engraftment and enhanced susceptibility to human immunodeficiency virus type 1 infection in NOD/LtSz-scid/scid mice. J Infect Dis. 1995;172:974-982.
11. Yoshino H, Ueda T, Kawahata M, et al. Natural killer cell depletion by anti-asialo GM1 antiserum treatment enhances human hematopoietic stem cell engraftment in NOD/Shi-scid mice. Bone Marrow Transplant. 2000;26:1211-1216.
12. Ueda T, Tsuji K, Yoshino H, et al. Expansion of human NOD/SCID-repopulating cells by stem cell factor, Flk2/Flt3 ligand, thrombopoietin, IL-6, and soluble IL-6 receptor. J Clin Invest. 2000;105: 1013-1021.
13. Ueda T, Yoshino H, Kobayashi K, et al. Hematopoietic repopulating ability of cord blood CD34(+) cells in NOD/Shi-scid mice. Stem Cells. 2000;18: 204-213.
14. Kollet O, Peled A, Byk T, et al. β2 microglobulin-deficient (B2m(null)) NOD/SCID mice are excellent recipients for studying human stem cell function. Blood. 2000;95:3102-3105.
15. Glimm H, Eisterer W, Lee K, et al. Previously undetected human hematopoietic cell populations with short-term repopulating activity selectively engraft NOD/SCID-β2 microglobulin-null mice. J Clin Invest. 2001;107:199-206.
16. Ito M, Hiramatsu H, Kobayashi K, et al. NOD/SCID/γ(c)(null) mouse: an excellent recipient mouse model for engraftment of human cells. Blood. 2002;100:3175-3182.
17. Noguchi M, Yi H, Rosenblatt HM, et al. Interleukin-2 receptor gamma chain mutation results in X-linked severe combined immunodeficiency in humans. Cell. 1993;73:147-157.
18. Puck JM, Deschenes SM, Porter JC, et al. The interleukin-2 receptor gamma chain maps to Xq13.1 and is mutated in X-linked severe combined immunodeficiency, SCIDX1. Hum Mol Genet. 1993;2:1099-1104.
19. Yahata T, Ando K, Nakamura Y, et al. Functional human T lymphocyte development from cord blood CD34(+) cells in nonobese diabetic/Shi-scid, IL-2 receptor gamma null mice. J Immunol. 2002;169:204-209.
20. Koyanagi Y, Tanaka Y, Kira J, et al. Primary human immunodeficiency virus type 1 viremia and central nervous system invasion in a novel hu-PBL–immunodeficient mouse strain. J Virol. 1997;71:2417-2424.
21. Lichtenfels R, Biddison WE, Schulz H, Vogt AB, Martin R. CARE-LASS (calcine-release-assay), an improved fluorescence-based test system to measure cytotoxic T lymphocyte activity. J Immunol Methods. 1994;172:227-239.
22. Williams NS, Klem J, Puzanov IJ, et al. Natural killer cell differentiation: insights from knockout and transgenic mouse models and in vitro systems. Immunol Rev. 1998;165:47-61.
23. Cooper MA, Bush JE, Fehniger TA, et al. In vivo evidence for a dependence on interleukin 15 for survival of natural killer cells. Blood. 2002;100: 3633-3638.
24. Whiteside TL, Herberman RB. The biology of human natural killer cells. Ann Ist Super Sanita. 1990;26:335-348.
25. Peault B, Weissman IL, Baum C, McCune JM, Tsukamoto A. Lymphoid reconstitution of the human fetal thymus in SCID mice with CD34+ precursor cells. J Exp Med. 1991;174:1283-1286.
26. Kollmann TR, Kim A, Zhuang X, Hachamovitch M, Goldstein H. Reconstitution of SCID mice with human lymphoid and myeloid cells after transplantation with human fetal bone marrow without the requirement for exogenous human cytokines. Proc Natl Acad Sci U S A. 1994;91:8032-8036.
27. Tournoy KG, Depraetere S, Meuleman P, Leroux-Roels G, Pauwels RA. Murine IL-2 receptor beta chain blockade improves human leukocyte engraftment in SCID mice. Eur J Immunol. 1998;28: 3221-3230.
28. Dao MA, Pepper KA, Nolta JA. Long-term cytokine production from engineered primary human stromal cells influences human hematopoiesis in an in vivo xenograft model. Stem Cells. 1997;15: 443-454.
29. Martin LH, Calabi F, Lefebvre FA, Bilsland CA, Milstein C. Structure and expression of the human thymocyte antigens CD1a, CD1b, and CD1c. Proc Natl Acad Sci U S A. 1987;84:9189-9193.
30. Tary-Lehmann M, Lehmann PV, Schols D, Roncarolo MG, Saxon A. Anti-SCID mouse reactivity shapes the human CD4+ T cell repertoire in hu-PBL-SCID chimeras. J Exp Med. 1994;180:1817-1827.
31. Hozumi N, Gorczynski R, Peters W, Sandhu JS. A SCID mouse model for human immune response and disease. Res Immunol. 1994;145: 370-379.
32. Pflumio F, Lapidot T, Murdoch B, Patterson B, Dick JE. Engraftment of human lymphoid cells into newborn SCID mice leads to graft-versus-host disease. Int Immunol. 1993;5:1509-1522.
33. Sanchez M, Alfani E, Visconti G, Passarelli AM, Migliaccio AR, Migliaccio G. Thymus-independent T-cell differentiation in vitro. Br J Haematol. 1998; 103:1198-1205.
34. Robin C, Bennaceur-Griscelli A, Louache F, Vainchenker W, Coulombel L. Identification of human T-lymphoid progenitor cells in $CD34^+$ $CD38^{low}$ and $CD34^+$ $CD38^+$ subsets of human cord blood and bone marrow cells using NOD-SCID fetal thymus organ cultures. Br J Haematol. 1999;104:809-819.
35. Weekx SF, Snoeck HW, Offner F, et al. Generation of T cells from adult human hematopoietic stem cells and progenitors in a fetal thymic organ culture system: stimulation by tumor necrosis factor-α. Blood. 2000;95:2806-2812.
36. Zhao Y, Swenson K, Sergio JJ, Sykes M. Pig MHC mediates positive selection of mouse $CD4^+$ T cells with a mouse MHC-restricted TCR in pig thymus grafts. J Immunol. 1998;161:1320-1326.

Development of both human connective tissue-type and mucosal-type mast cells in mice from hematopoietic stem cells with identical distribution pattern to human body

Naotomo Kambe, Hidefumi Hiramatsu, Mika Shimonaka, Hisanori Fujino, Ryuta Nishikomori, Toshio Heike, Mamoru Ito, Kimio Kobayashi, Yoshito Ueyama, Norihisa Matsuyoshi, Yoshiki Miyachi, and Tatsutoshi Nakahata

The transplantation of primitive human cells into sublethally irradiated immunodeficient mice is the well-established in vivo system for the investigation of human hematopoietic stem cell function. Although mast cells are the progeny of hematopoietic stem cells, human mast cell development in mice that underwent human hematopoietic stem cell transplantation has not been reported. Here we report on human mast cell development after xenotransplantation of human hematopoietic stem cells into nonobese diabetic severe combined immunodeficient (NOD/SCID)/γ_c^{null} (NOG) mice with severe combined immunodeficiency and interleukin 2 (IL-2) receptor γ-chain allelic mutation. Supported by the murine environment, human mast cell clusters developed in mouse dermis, but they required more time than other forms of human cell reconstitution. In lung and gastric tract, mucosal-type mast cells containing tryptase but lacking chymase located on gastric mucosa and in alveoli, whereas connective tissue-type mast cells containing both tryptase and chymase located on gastric submucosa and around major airways, as in the human body. Mast cell development was also observed in lymph nodes, spleen, and peritoneal cavity but not in the peripheral blood. Xenotransplantation of human hematopoietic stem cells into NOG mice can be expected to result in a highly effective model for the investigation of human mast cell development and function in vivo. (Blood. 2004;103: 860-867)

Introduction

Mast cells are recognized as the principal cells which initiate immunoglobulin E (IgE)–dependent immediate hypersensitivity and also as the cells which contribute to innate immunity and tissue remodeling.[1,2] There are 2 phenotypically distinct mast cell subpopulations in rodents: connective tissue-type mast cells (CTMCs) and mucosal-type mast cells (MMCs). These populations differ in location, cell size, staining characteristics, ultrastructure, mediator content, and T-cell dependency.[3] Proliferation of rodent MMCs is dependent on T-cell–derived cytokines,[3,4] whereas that of CTMCs is supported by stem cell factor (SCF). In humans, mast cells are distinguished on the basis of their protease composition,[5,6] MC_{TC} contains tryptase and chymase in its granules and is predominant in skin and intestinal submucosa, like CTMCs in rodents. MC_T also contains tryptase, but lacks chymase, and is predominant in the alveolar .wall and gastric mucosa, similar to MMCs in rodents. Human mast cells were reported to develop only under the influence of SCF, but T-cell–derived interleukin 3 (IL-3) has little affect on their differentiation.[7] Recently, human intestinal mast cells were reported to respond to IL-3 by enhancing their growth,[8] but SCF is still an indispensable factor for human mast cells. Mast cells are the progenies of hematopoietic stem cells (HSCs).[9,10] In mice, the progenitor cells capable of becoming mast cells leave the bone marrow and enter the circulation but complete their differentiation into mast cells only after arriving in peripheral tissues such as lung, bowel, and skin.[10,11] Unfortunately, the developmental mechanism of human mast cells remains far less clear, possibly because the lack of an appropriate in vivo assay system.

The transplantation of primitive human cells into immunedeficient C.B-17-Prkdc^{scid} *(scid)*[12,13] and into NOD/LtSz-*scid* or NOD/Shi-*scid* (nonobese diabetic severe combined immunodeficient [NOD/SCID]) mice[14,15] is thought to constitute an appropriate functional in vivo system for human HSCs. However, it has been suggested that residual natural killer (NK) cell activity in NOD/SCID mice might interfere with engraftment.[16,17] Recently, we developed NOD/SCID/γ_c^{null} (NOG) mice by backcrossing IL-2 receptor γ-chain deficient (γ_c^{null}) mice to NOD/Shi-*scid* mice.[18] Compared with NOD/SCID mice treated with anti-NK cell antibody[17] and NOD/SCID/β_2 microglobulin^{null} mice,[19,20] both of which were established for reducing residual NK cell activity, the newly developed NOG mice were superior in terms of efficiencies of human HSC engraftment, because they lack NK cell activity and show reduced interferon γ production from dendritic cells.[18] In addition, human CD3$^+$ T cells can be generated and matured from human HSCs in NOG but not in other mice.[21,22] These results encouraged us to check human mast cell development in NOG

From the Department of Pediatrics and Dermatology, Kyoto University Graduate School of Medicine, Kyoto, Japan; Central Institute for Experimental Animals, Kawasaki, Japan; and the Department of Pathology, Tokai University School of Medicine, Isehara, Japan.

Submitted April 14, 2003; accepted September 17, 2003. Prepublished online as *Blood* First Edition Paper, October 2, 2003; DOI 10.1182/blood-2003-04-1160.

Supported by grant 14770405 (N.K.) and Grant-in-Aid for Creative Scientific Research (S) 13GS0009 (T.N.) from the Ministry of Education, Science, Sports, and Culture, Japan, as well as the Long-Range Research Initiative grant CS05-07 (Y.M.) from the Japan Industry Association.

Reprints: Tatsutoshi Nakahata, Department of Pediatrics, Kyoto University Graduate School of Medicine, 54 Kawahara-cho, Shogoin, Sakyo-ku, Kyoto 606-8507, Japan; e-mail: tnakaha@kuhp.kyoto-u.ac.jp.

The publication costs of this article were defrayed in part by page charge payment. Therefore, and solely to indicate this fact, this article is hereby marked "advertisement" in accordance with 18 U.S.C. section 1734.

mice, even though there are no reports of mast cell development after human HSC transplantation into mice.

This is, therefore, the first report of human mast cell development in mice after transplantation of human HSCs, with NOG mice as recipients. Moreover, development of human mast cells in NOG mice was supported by the murine environment, and, depending on their protease compositions, the distribution of human mast cells was similar to that in the human body.

Materials and methods

Mice, human cell preparation, and xenotransplantation

NOG mice were established at the Central Institute of Experimental Animals (Kawasaki, Japan) by backcrossing γ_c^{null} mice to NOD/Shi-*scid* mice, as reported previously.[18] The mice were shipped to the animal facility of Kyoto University (Kyoto, Japan) and kept under specific pathogen-free conditions in accordance with the facility's guideline.

Human cord blood was collected from healthy full-term deliveries after obtaining informed consent. Mononuclear cells were isolated on Ficoll-Hypaque (Pharmacia, Uppsala, Sweden) after phagocyte depletion with silica (ImmunoBiological Laboratories, Gunma, Japan).[23] $CD34^+$ cell fractions were further isolated by using AutoMACS (Miltenyi Biotec, Bergisch Gladbach, Germany). After the enrichment, assessment of their purity by flow cytometry showed that approximately 95% of the cells were $CD34^+$ cells. In the experiments using lineage-depleted cells ($lin^-/CD34^+$ cells), cord blood mononuclear cells were treated with StemSep (Stem Cell Technologies, Vancouver, Canada), followed by $CD34^+$ selection.

Xenotransplantation of purified human cells into NOG mice was also described previously.[18,21] Mice were irradiated at 8 to 12 weeks of age with 240 cGy. Enriched $CD34^+$ cells (50 000) were injected intravenously through the tail vein. After the transplantation, mice were given sterile water containing prophylactic neomycin sulfate (Invitrogen, Carlsbad, CA). The experimental protocol was approved by the Human Studies Internal Review Board at Kyoto University (no. 322).

Flow cytometry

Human cell development in NOG mice was periodically monitored with a flow cytometer (FACS Calibur; BD Cytometry, San Diego, CA) with fluorescein isothiocyanate (FITC)–conjugated antihuman CD45 monoclonal antibody (mAb) and allo-phycocyanin (APC)–conjugated antimouse CD45 mAb (BD Pharmingen, San Diego, CA), as previously reported.[18,21] The lineage analysis was performed with APC-conjugated antihuman CD45; phycoerythrin (PE)–conjugated anti-CD3, anti-CD33 (BD Pharmingen), and anti-CD203c mAb which recognized both human mast cells and basophils[24,25]; PC5-conjugated anti-CD19, anti-CD56, and anti-Kit (CD117) mAb (Immunotech, Marseille, France): and biotin-conjugated anti-CD123 (IL-3 receptor α-chain) and streptavidin-FITC (BD Pharmingen).

Murine mast cell determination

Tissue samples were frozen in O.C.T. Tissue-Tek compound (Miles Labs, Elkhart, IN) or fixed in 10% buffered formalin or Carnoy solution (60% ethanol, 30% chloroform, and 10% acetic acid). Those sections were stained with acidic toluidine blue. Carnoy fixed preparations were used for safranin-O and Alcian blue staining.

To collect mast cells from the peritoneal cavity, 5 mL prewarmed Hanks balanced salt solution containing 1% fetal calf serum was injected into the mouse peritoneal cavity. The abdomen was gently massaged for 1 minute, after which the peritoneal cavity was carefully opened, and the fluid containing peritoneal cells was collected with a pipette. One part of the collected cell suspension was used for direct counting of living cells, and the remaining cells were used for staining with toluidine blue or with safranin-O and Alcian blue on the cytospin preparations and for cytometry. On the cytospin preparation, a proportion of the positively stained cells among the 200 nucleated cells was determined.

Immunochemistry

To detect human mast cells, acetone-fixed frozen sections were blocked with donkey serum before incubation with antihuman CD45 mAb (Nichirei, Tokyo, Japan) and then incubated with Cy3-conjugated 2nd Ab (Jackson, West Grove, PA), FITC-conjugated avidin bound to mast cells,[26,27] and Hoechst 33342 (Molecular Probes, Eugene, OR). Specificity of avidin binding to mast cells was confirmed with both human and mouse tissue preparations from skin, lung, and gastric stomach.

We used acetone-fixed frozen sections for chymase, because the routinely used Carnoy solution reduces the number of $chymase^+$ cells.[28] Antihuman chymase mAb (Chemicon, Temecula, CA) labeled slides were stained with alkaline phosphatase (AP)–conjugated 2nd Ab (Vector, Burlingame, CA). For tryptase, formalin-fixed paraffin-embedded sections and methanol-fixed cytospin preparations were incubated with antitryptase mAb (Chemicon) and with AP-conjugated 2nd Ab. The color was developed with naphthol AS-BI/new fuchsin. In some experiments, biotin-conjugated antichymase mAb-labeled cells were incubated with horseradish peroxidase–conjugated streptavidin, and the color was developed with 3-amino-9-ethylcabbazole (Vector). The cells were sequentially labeled with AP-conjugated antitryptase mAb, and the color was developed with fast blue substrate (Vector). We used healthy parts of skin obtained after mastectomy as positive controls.

For SCF distribution in NOG mouse skin, we sequentially incubated acetone-fixed frozen sections with antimouse SCF polyclonal Ab (R&D systems, Minneapolis, MN) and Cy3-conjugated 2nd Ab (Jackson) and observed with a confocal laser microscopy (Olympus).

RNA purification and RT-PCR (reverse transcription–polymerase chain reaction)

Cellular total RNA was isolated with the phenol/guanidine isothiocyanate method using a Trizol reagent (Invitrogen) and reverse-transcribed to complementary (cDNA) with oligo dT primers and SuperScript Synthesis System (Invitrogen). Reaction mixtures were amplified with 0.2 U Taq polymerase (Sigma) using 25 cycles for glyceraldehyde-3-phosphate dehydrogenase (G3PDH) and 40 cycles for others under the following conditions: denaturation at 95°C for 30 seconds, annealing at 55°C for 30 seconds, and extension at 72°C for 30 seconds. Oligonucleotide primers for SCF which recognized both human and mouse SCF, 5′-TCTTCAGCTGCTCCTATTT-3′ and 5′-ACTGCTACTGCTGTCATTC-3′; human tryptase, 5′-GGAAAACCACATTTGTGACG-3′ and 5′-ATTCACCTTGCACACAGGG-3′; and human chymase, 5′-AAGGAGAAAGCCAGCCTGACC-3′ and 5′-TCCGACCGTCCATAGGATACG-3′ were synthesized.

To evaluate the species origin of SCF, PCR products were purified with the QIAquick PCR purification kit (Qiagen, Valencia, CA) and digested for 1 hour with restriction enzymes, *XmaI* and *NsiI*. Mouse keratinocyte Pam212 and human keratinocyte DJM-1 were positive controls.

Human mast cell culture in vitro

Human cord blood $CD34^+$ cells were cultured in AIM-V medium (Invitrogen) with either human SCF (Amgen, Thousand Oaks, CA) or murine SCF (Kirin Brewery, Gunma, Japan) at concentration of 10 ng/mL (suboptimal) or 100 ng/mL (optimal), as described previously but with a minor modification.[29-31] During the first week, 50 ng/mL human IL-6 (Kirin Brewery) was also added. Flow cytometry at the constant flow rate was used to assess viable cell number with propidium iodide and mast cell percentage with anti-Kit mAb.

Statistical analysis

Data are presented as the mean ± SD values. Statistical significance was determined with the Student t test, and $P < .01$ was considered significant.

Results

Murine mast cell distribution in NOG mice

Compared with age-matched control B6 mice, the dermis of 12-week-old NOG mice (n = 6) has a normal concentration of mast cells (Figure 1A-B), but, surprisingly, in the skin of 20-week-old NOG mice (n = 6), we observed a substantial number of toluidine blue$^+$ cells in the upper dermis (Figure 1C-D). The pathologic findings also showed epidermal hyperplasia.

Murine mast cells collected from the peritoneal cavity were safranin$^+$ CTMCs, as from the dermis. The number of peritoneal mast cells from 12-week-old NOG mice ($0.51 \pm 0.07 \times 10^6$ cells/mouse, mean ± SD values from 6 mice) was not different from that from control B6 mice ($0.49 \pm 0.05 \times 10^6$ cells/mouse). Although peritoneal mast cells in B6 mice had a tendency to increase in number as the mice became older, 20-week-old NOG mice had significantly fewer peritoneal mast cells ($0.28 \pm 0.05 \times 10^6$ cells/mouse) than did 20-week-old B6 mice ($1.02 \pm 0.57 \times 10^6$ cells/mouse, n = 6) ($P < .01$). Figure 1E shows toluidine blue staining of the mesentery from 20-week-old NOG mice, and Figure 1F shows safranin-O staining of peritoneal cells, also from 20-week-old NOG mice.

In addition, we checked mast cells in lung and gastric tract, where MMCs were predominantly distributed. The lungs showed no mast cell at the alveoli (Figure 1G) but a few mast cells, which were safranin$^+$ CTMCs, around major airways (Figure 1H). In the gastric stomach, mast cells were distributed in both submucosa and mucosa (Figure 1I-K). Mast cells in the submucosa were safranin$^+$ CTMCs (arrowheads in Figure 1I-J), whereas unexpectedly safranin-negative, Alcian blue$^+$ MMCs were identified in gastric mucosa (arrows in Figure 1I,K), even though NOG mice lack T cells because of γ_c^{null} mutation. The number of mast cells in the lung and gastric tract of the control B6 mice and the older NOG mice had not changed.

In NOG mice, lymph nodes could hardly be identified without human HSC transplantation: only 2 lymph nodes at the axillaries and one at the mesenteric region of 6 mice. Pathologic examination of these identified lymph nodes showed a small number of mast cells located in the connective tissue at the capsule and an even smaller number of mast cells at the trabecula of the lymph node, and none in the cortex or medulla (Figure 1L). They were all safranin$^+$ CTMCs (data not shown). In spleen of NOG mice, mast cells were present in the connective tissue of the trabecula, as shown with arrows in Figure 1M. Again, they were all safranin$^+$ CTMCs (data not shown). Except for the ease of finding lymph nodes from control B6 mice, the number and histologic distribution of mast cells in lymph nodes and spleen of 12-week-old NOG mice were not different from those of the control B6 mice and the older NOG mice.

Human mast cell development in mouse skin

Four weeks after transplantation of cord blood CD34$^+$ cells, human CD45$^+$ cells were detected in NOG mouse peripheral blood, in which CD33$^+$ myeloid cells were predominant, and CD19$^+$ B cells and CD56$^+$ NK cells were also present (Figure 2). Human CD45$^+$ cells gradually increased, and 12 weeks after transplantation, we also observed abundant human CD3$^+$ T cells in NOG mice, in agreement with previous study.[18]

To identify mast cell development after human CD34$^+$ cell transplantation into NOG mice, we first tried to detect tryptase and chymase messenger RNA (mRNA) expression in the skin. Four weeks or 8 weeks after xenotransplantation (n = 3), this expression was hardly detectable. Twelve weeks after the transplantation (n = 3), however, human mast cell-specific protease expression was identified in NOG mouse skin (Figure 3A). At this time, chymase mRNA was more prominent than tryptase mRNA.

In addition, we stained skin sections with antihuman CD45 mAb, which did not react to NOG mice not receiving transplants (data not shown). Four weeks or 8 weeks after xenotransplantation (n = 3), unexpectedly we observed human CD45$^+$ cells mainly in

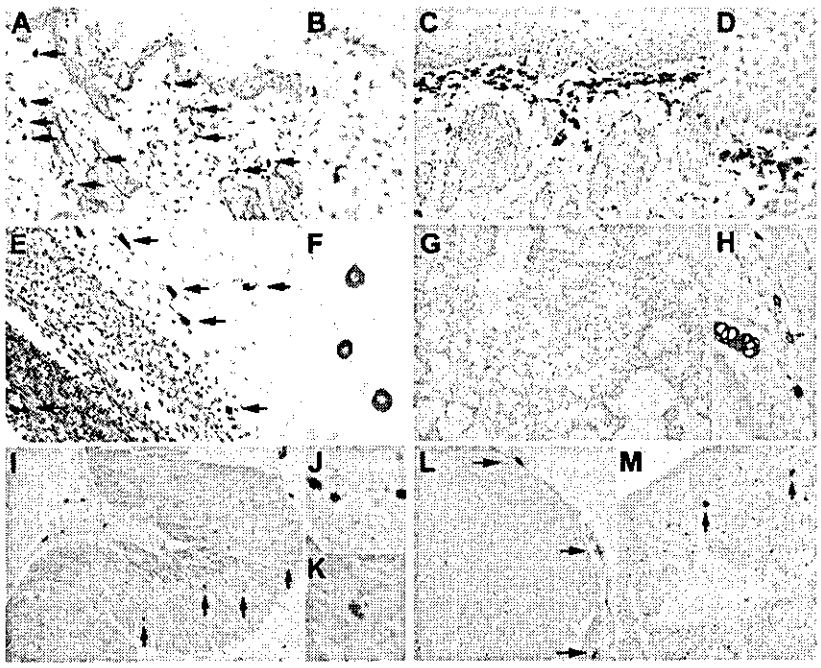

Figure 1. Murine mast cell distribution in NOG mice. (A-D) Toluidine blue staining of the skin of NOG mice. Thin frozen sections from 12-week-old (A-B) and 20-week-old (C-D) NOG mice were stained with acidic toluidine blue. Arrows in the picture from 12-week-old NOG mice (A) indicate metachromatically stained cells. The upper dermis of 20-week-old NOG mice shows bandlike proliferation of toluidine blue$^+$ cells and hyperplasia of epidermis. Magnification, × 200 (A,C) and × 400 (B,D). (E) Toluidine blue staining of mesentery of 20-week-old NOG mice, and arrows indicate mast cells. Magnification × 200. (F) Safranin-O staining of peritoneal cells obtained from 20-week-old NOG mice. Magnification, × 400. (G-K) Alcian blue and safranin-O staining in Carnoy fixed preparations from 20-week-old NOG mice. In lung, a few safranin$^+$ CTMCs were recognized around major airways (H), whereas safranin-negative, Alcian blue$^+$ MMCs were not observed in alveoli (G). In the gastric stomach, NOG mice showed safranin$^+$ CTMCs in the submucosa (arrowheads in I and image with hypermagnification in J), and safranin-negative, Alcian blue$^+$ MMCs in mucosa (arrows in I and image with hypermagnification in K). Magnification, × 100 (G,I), × 200 (H), and × 400 (J-K). (L-M) Toluidine blue staining of Carnoy fixed preparations from lymph node (L) and spleen (M) from 20-week-old NOG mice. Mast cells located only at the capsule of the lymph nodes. In the spleen, a few mast cells were present as shown with arrows in M. Magnification, × 200 (L-M).

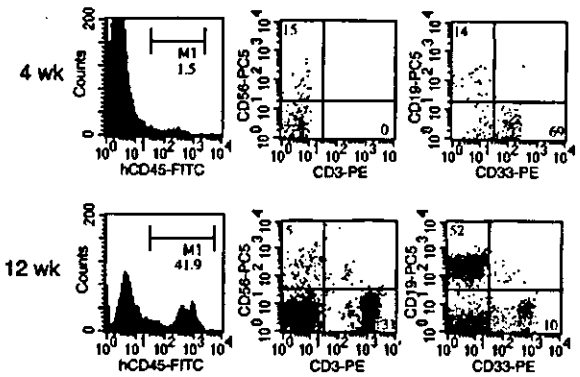

Figure 2. Representative flow cytometric analysis of peripheral blood from NOG mice after HSC transplantation. Four weeks after the transplantation, less than 2% of the cells were human CD45, in which CD33$^+$ myeloid cells were predominant, and CD19$^+$ B cells and CD56$^+$ NK cells were also present. Twelve weeks after the transplantation, more than 40% cells were replaced by human CD45$^+$ cells, among which abundant human CD3$^+$ T cells were identified.

the upper dermis and some in the basal layer of the epidermis. However, none of these human CD45$^+$ cells were positive for FITC-avidin, indicating they were not mast cells. Twelve weeks after the transplantation (n = 8), finally we could detect a small number of avidin-FITC and human CD45 double-positive mast cells in the dermis (Figure 3B). Then, the number of double-positive human mast cells gradually but focally increased to produce clusters in the dermis of NOG mice (Figure 3C).

Next, we checked the presence of human mast cell-specific tryptase and chymase by immunochemical staining. Staining the skin of NOG mice not receiving transplants with antihuman chymase mAb showed no positive cells, confirming that there was no cross-reaction to mouse mast cells (data not shown). More than 12 weeks after xenotransplantation into NOG mice, we recognized human chymase$^+$ cells focally in the dermis, and after 24 weeks (n = 6), some mast cell clusters consisted of more than 100 human chymase$^+$ cells (Figure 3D-E). The number and size of the clusters consisting of chymase$^+$ cells in NOG mouse skin differed even among the specimens obtained from the same mouse. As shown in Figure 3E, in some areas of NOG mouse skin, proliferated mast cells consisted of only chymase$^+$ human mast cells but not murine mast cells. We counted the mast cells in the area under 500 μm of skin surface and above the sebaceous gland of the dermis and found that the number of human mast cells in the area consisting of only chymase$^+$ cells (38.0 ± 8.4 cells/500 μm, mean ± SD values from 5 different preparations) and that of mouse mast cells in the area consisting of only nonstained granulated cells (39.8 ± 3.9) was almost the same 24 weeks after the transplantation (Figure 3G).

At the same time, we recognized cells showing strong positive reaction for human tryptase in the upper dermis of NOG mice on the formalin-fixed preparations. These cells were recognized only more than 12 weeks after xenotransplantation (data not shown).

Differentiation into mast cells from HSCs

To confirm de novo generation of human mast cells from HSCs, we transplanted lineage-depleted cells into NOG mice and analyzed the skin, lung, and stomach 4, 8, 12, and 20 weeks after the transplantation (n = 3 for each time point). But the time course of mast cell development in those tissues after transplantation with lin$^-$/CD34$^+$ cells was the same as that with whole CD34$^+$ cells.

Human mast cell development supported by mouse SCF

To identify what kind of environment that supports human mast cell development in NOG mouse skin, we examined SCF production. Restriction enzymes could identify the species origin of amplified PCR-products: *Xma*I cut human products to 137 and 425 base pairs (bp), whereas *Nsi*I cut murine products to 257 and 305 bp (Figure 4A). Although mast cells themselves can produce SCF,[32] and we actually detected SCF derived from in vitro–cultured human mast cells, digestion of PCR products suggested that murine SCF was dominant in the skin of NOG mice even when human mast cells had been reconstituted after the successful transplantation of human CD34$^+$ cells (Figure 4B). We got the same results

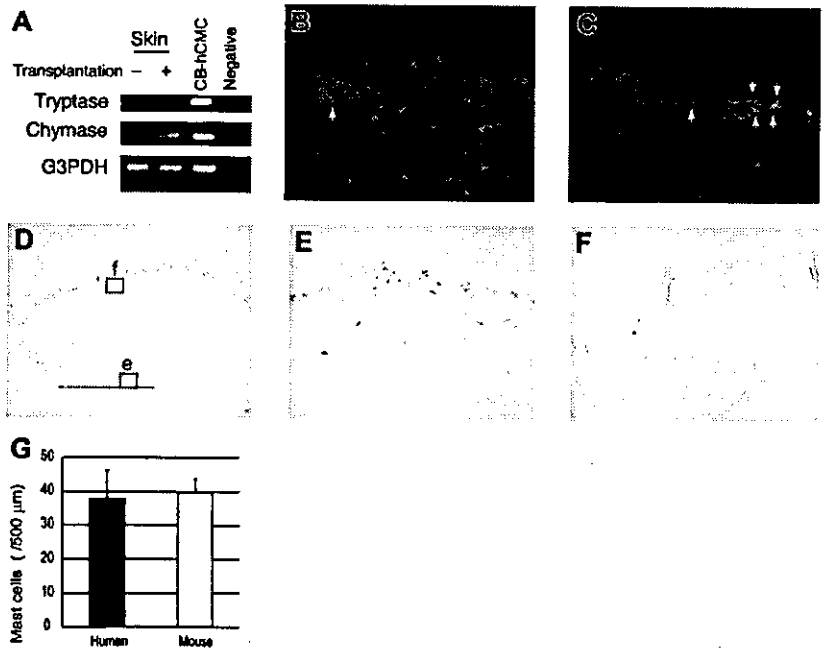

Figure 3. Human mast cell development in the mouse skin. (A) RT-PCR analysis for tryptase and chymase mRNA expression. The skin of NOG mice 12 weeks after the transplantation of human CD34$^+$ cells expressed human mast cell-specific tryptase and chymase mRNA. CB-hCMC indicates cord blood-derived human cultured mast cells. (B-C) Acetone-fixed frozen sections of NOG mouse skin 12 weeks (B) and 20 weeks (C) after the transplantation of human cord blood CD34$^+$ cells were stained for human CD45 (red fluorescent with Cy3), mast cells (yellowish green with FITC-avidin), and nuclei (blue with Hoechst 33342). Arrows indicate human CD45$^+$ mast cells, which are stained orange. Magnification, × 200. (D-F) Human MC specific chymase$^+$ cells in the mouse skin. Acetone-fixed frozen sections of NOG mouse skin 24 weeks after the transplantation were stained with antihuman chymase mAb. Human chymase$^+$ cells proliferated focally in the upper dermis (e), represented by the bar bellows, whereas in other lesions on the same samples nonstained granulated cells were located in the upper dermis (f). Magnification, × 12.5 (D) and ⁄ 200 (E-F). (G) The number of chymase$^+$ human mast cells and nonstained granulated mouse mast cells in NOG mouse skin 24 weeks after the transplantation. The number of human and mouse mast cells supported by mouse dermis was almost identical. Bar graphs display mean ± SD values from 5 different preparations.

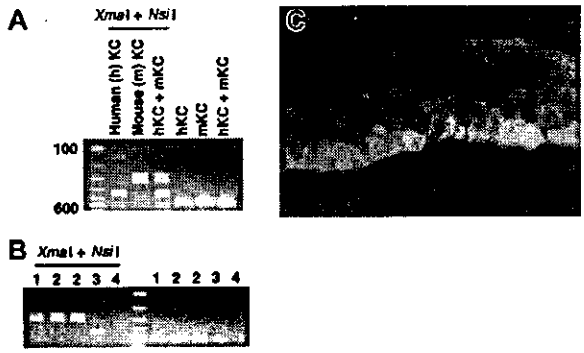

Figure 4. SCF expression in the mouse skin. (A) Control study for PCR and restriction enzymes. Templates from human DJM-1 and mouse Pam212 keratinocytes were amplified after PCR and then digested with *Xmal* and *Nsil*. Human SCF products were cut to 137 and 425 bp and mouse SCF products to 257 and 305 bp. KC indicates keratinocytes. (B) Human mast cell development in NOG mouse skin was predominantly supported by mouse SCF. Expected 562-bp bands were observed after PCR reaction. The digestion patterns with *Xmal* and *Nsil* suggested the main source of SCF in the skin was mouse-derived SCF even after the xenotransplantation. 1 indicates NOG mouse not receiving transplant; 2, NOG mouse 12 weeks after xenotransplantation; 3, in vitro–derived cultured human mast cells from cord blood; and 4, negative control. The findings were similar when cDNA template from NOG mouse skin was used 8 weeks and 20 weeks after the transplantation. (C) Mouse SCF protein distribution in the NOG mouse skin. SCF localized in a physiologically cytoplasmic pattern in the epidermis. Magnification × 400.

using any of the cDNA samples prepared from the NOG mice 8 weeks, 12 weeks, and 20 weeks after the xenotransplantation.

SCF has 2 phenotypes depending on its distribution pattern. It has been reported that in patients with cutaneous mastocytosis, SCF protein shifts from a cytoplasmic pattern to an intercellular pattern and represents a secretion phenotype.[33] In NOG mice, SCF was mainly produced at the epidermis where SCF localized in cytoplasm represents a physiologic phenotype (Figure 4C). This finding was similar to the findings observed before or after the transplantation of human CD34$^+$ cells into the mice.

Our result suggests that murine SCF under normal conditions supported human mast cell development in NOG mouse. We also checked whether murine SCF could support human mast cell development from cord blood by using an in vitro culture system. Six weeks after the cultivation, more mast cells had developed with murine SCF than human SCF (Figure 5), indicating that murine SCF can support human mast cell development from HSCs even more efficiently than human SCF.

Lung and gastric stomach

To determine human mast cell development in organs other than skin, we examined lung and gastric stomach, where MC_T was dominant in humans. Twelve weeks after transplantation of human cord blood CD34$^+$ cells, we could detect both tryptase and chymase mRNA in lung and gastric stomach of NOG mice (Figure 6A). In contrast to the skin, the intensity of tryptase mRNA was stronger than that of chymase mRNA in lung.

Although murine MMCs were sensitive to formalin and invisible on formalin-fixed preparations before the transplantation (data not shown), in the formalin-fixed specimens from lung 20 weeks after xenotransplantation, a small number of toluidine blue$^+$ cells, 3 to 12 cells, was observed in the frontal section of the unilateral lung (n = 4). In sequential sections, we confirmed most of the toluidine blue$^+$ cells were strongly positive for human tryptase. Human chymase$^+$ cells were seen only in the connective tissue around major airways (Figure 6B) and in the submucosal tissue under the esophagus (data not shown). In gastric stomach, we could detect formalin-resistant toluidine blue$^+$ cells in both gastric mucosa and submucosa, which were identically stained by human tryptase in sequential sections (Figure 6C). However, chymase$^+$ cells were located only in submucosa where they showed focal proliferation in clusters.

Bone marrow and peripheral blood

Although neither tryptase$^+$ cells nor toluidine blue$^+$ cells could be detected on smear preparations periodically obtained from bone marrow and peripheral blood (data not shown), analysis of more than 20 000 cells by flow cytometry identified a small number of CD203c$^+$ cells in human CD45$^+$ cells from the bone marrow (3.4% in human CD45$^+$ cells) and peripheral blood (1.2% in human CD45$^+$ cells) 20 weeks after the xenotransplantation (Figure 7A). In bone marrow, most of these CD203c$^+$ cells also strongly expressed Kit (CD117), suggesting they were human mast cells. A small portion of Kit-negative and IL-3 receptor α-chain (CD123) weakly positive cells were also observed in CD203c$^+$ cells, suggesting the presence of human basophils. However, all CD203c$^+$ cells in the peripheral blood were negative for Kit but expressed IL-3 receptor, indicating that human basophils were reconstituted from the transplanted human CD34$^+$ cells and circulated in NOG mice (n = 4).

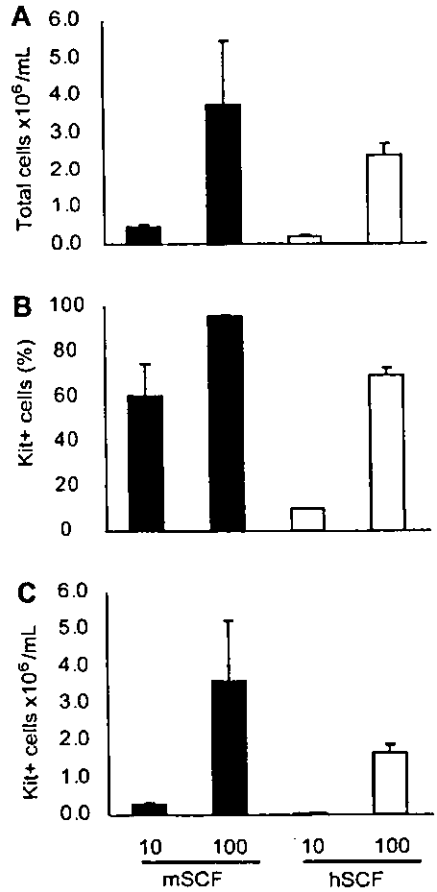

Figure 5. Mouse SCF effectively supports human mast cell development in vitro. Human cord blood CD34$^+$ cells were cultured with suboptimal (10 ng/mL) and optimal (100 ng/mL) doses of recombinant SCF. The number of mast cells (C) after 6 weeks of culture was assessed in terms of the total number of the viable cells (A) and the Kit$^+$ percentage (B) determined by flow cytometric analysis. Bar graphs display mean ± SD values from 3 independent experiments.